



**INVESTIGATION OF THE EFFECTS OF TI AND
ZR ELEMENTS ADDED TO 316L STAINLESS
STEEL ON MICROSTRUCTURE, MECHANICAL,
WEAR AND CORROSION PROPERTIES**

**2024
MASTER THESIS
MECHANICAL ENGINEERING**

Meftah Abdallah ABUSHAALA

**Thesis Advisors
Assoc. Prof. Dr. Harun ÇUĞ
Prof. Dr. Mehmet Akif ERDEN**

**INVESTIGATION OF THE EFFECTS OF TI AND ZR ELEMENTS ADDED
TO 316L STAINLESS STEEL ON MICROSTRUCTURE, MECHANICAL,
WEAR AND CORROSION PROPERTIES**

Meftah Abdallah ABUSHAALA

Thesis Advisors

Assoc. Prof. Dr. Harun ÇUĞ

Prof. Dr. Mehmet Akif ERDEN

T.C.

Karabuk University

Institute of Graduate Programs

Department of Mechanical Engineering

Prepared as

Master Thesis

KARABUK

January 2024

I certify that in my opinion the thesis submitted by Meftah Abdallah ABUSHAALA titled “INVESTIGATION OF THE EFFECTS OF TI AND ZR ELEMENTS ADDED TO 316L STAINLESS STEEL ON MICROSTRUCTURE, MECHANICAL, WEAR AND CORROSION PROPERTIES ” is fully adequate in scope and in quality as a thesis for the degree of Master of Science.

Assoc. Prof. Dr. Harun ÇUĞ
.....

Thesis Advisor, Department of Mechanical Engineering

Prof. Dr. Mehmet Akif ERDEN
.....

Second Thesis Advisor, Department of Medical Engineering

This thesis is accepted by the examining committee with a unanimous vote in the Department of Mechanical Engineering as a Master of Science thesis. January 18, 2024

Examining Committee Members (Institutions)

Signature

Chairman : Assoc. Prof. Dr. Harun ÇUĞ (KBU)
.....

Member : Assoc. Prof. Dr. Mehmet AKKAŞ (KU)
.....

Member : Assoc. Prof. Dr. Hüseyin DEMİRTAŞ (KBU)
.....

The degree of Master of Science by the thesis submitted is approved by the Administrative Board of the Institute of Graduate Programs, Karabuk University.

Assoc. Prof. Dr. Zeynep ÖZCAN
.....

Director of the Institute of Graduate Programs

“I declare that all the information within this thesis has been gathered and presented in accordance with academic regulations and ethical principles and I have according to the requirements of these regulations and principles cited all those which do not originate in this work as well.”

Meftah Abdallah ABUSHAALA

ABSTRACT

M. Sc. Thesis

INVESTIGATION OF THE EFFECTS OF Ti AND Zr ELEMENTS ADDED TO 316L STAINLESS STEEL ON MICROSTRUCTURE, MECHANICAL, WEAR AND CORROSION PROPERTIES

Meftah Abdallah ABUSHAALA

Karabuk University

Institute of Graduate Programs

Department of Mechanical Engineering

Thesis Advisors:

Assoc. Prof. Dr. Harun ÇUĞ

Prof. Dr. Mehmet Akif ERDEN

January 2024, 77 pages

In this study, titanium (Ti) and zirconium (Zr) elemental powders were added separately and together synergistically in determined quantities (0.2, 0.5 and 1% by weight) using powder metallurgy (PM) technology into a 316 L stainless steel matrix. The powders used in the study were cold pressed sample molds prepared in accordance with ASTM E8M standards and were turned into blocks by cold pressing one-way under 750 MPa compression pressure. After the pressing process, the raw strength samples were sintered in an atmosphere-controlled tube furnace at 1310 °C in an argon atmosphere for two hours. The microstructure and mechanical properties of the produced PM steels were characterized using optical microscopy, tensile test and hardness test, density test, corrosion and wear test. The results showed that the sample with 316 L + 0.2 Ti +0.2 Zr added had the highest yield strength, tensile strength and

hardness strength. However, when more than 0.2% Ti was added to 316 L stainless steel and 0.2% Zr was added, a decrease in mechanical properties was observed. Again, the sample with the best wear performance was the sample to which 316 L + 0.2 Ti + 0.2 Zr was added.

Keywords : Powder metallurgy, 316L stainless steel, titanium; zirconium;
mechanical properties, microstructure, wear, corrosion.

Science Code : 91437

ÖZET

Yüksek Lisans Tezi

316L PASLANMAZ ÇELİKLERE EKLENEN Ti VE Zr ELEMENTLERİNİN MİKRO YAPI, MEKANİK, AŞINMA VE KOROZYON ÖZELLİKLERİ ÜZERİNDEKİ ETKİLERİNİN İNCELENMESİ

Meftah Abdallah ABUSHAALA

Karabük Üniversitesi

Lisansüstü Eğitim Enstitüsü

Makine Mühendisliği Anabilim Dalı

Tez Danışmanları:

Doç. Dr. Harun ÇUĞ

Prof. Dr. Mehmet Akif ERDEN

Ocak 2024, 77 sayfa

Bu çalışmada, 316 L paslanmaz çelik matris içerisine titanyum (Ti) ve zirkonyum (Zr) element tozları, toz metalurjisi (TM) teknolojisi kullanılarak belirlenen miktarlarda (ağırlıkça %0,2, 0,5 ve 1) ayrı ayrı ve birlikte sinerjistik olarak eklenmiştir. olarak eklendi. Çalışmada kullanılan tozlar ASTM E8M standartlarına uygun olarak hazırlanan soğuk pres numune kalıpları olup 750 MPa sıkıştırma basıncı altında tek yönlü soğuk preslenerek blok haline getirilmiştir. Presleme işleminden sonra ham mukavemet numuneleri atmosfer kontrollü tüp fırında 1310 °C sıcaklıkta argon atmosferinde iki saat sinterlenmiştir. Üretilen PM çeliklerin mikroyapısı ve mekanik özellikleri optik mikroskopi, çekme testi ve sertlik testi, yoğunluk testi, korozyon ve aşınma testi kullanılarak karakterize edildi. Sonuçlar, 316 L + 0,2 Ti +0,2 Zr ilave edilen numunenin en yüksek akma dayanımı, çekme dayanımı ve sertlik dayanımına sahip olduğunu gösterdi. Ancak 316 L paslanmaz çeliğe %0,2'den fazla Ti

eklendiğinde ve %0,2 Zr eklendiğinde mekanik özelliklerde azalma gözlenmiştir. Yine aşınma performansı en iyi olan numune 316 L + 0,2 Ti + 0,2 Zr ilave edilen numune olmuştur.

Anahtar Kelimeler : Toz metalurjisi, 316L paslanmaz çelik, titanyum, zirkonyum, mekanik özellikler, mikro yapı, aşınma, korozyon.

Bilim Kodu : 91437

ACKNOWLEDGMENT

First thanks, God Almighty, and later, my father and mother, for all their struggles from the day of my birth until this time. You are everything; I love you in God's love, and I also extend my sincere thanks to my wife, who has always been supportive of me in all circumstances. Thanks, and gratitude to my children, brothers, sisters, and friends. I am satisfied to thank all those who encouraged, directed, and contributed with me through my preparation of this thesis by denoting the needed references and resources in any phase of its phases, and I thank in particular my supervisors, Assoc. Prof. Dr. Harun ÇUĞ and Prof. Dr. Mehmet Akif ERDEN for my support and guiding me with advice and correction and for selecting the title and subject. My thanks also go to the administration of the Faculty of Engineering at the University of Karabuk in the Department of Mechanical Engineering for providing the best environment for teaching engineering sciences in the best conditions for science students.

CONTENTS

	<u>Page</u>
APPROVAL PAGE	ii
ABSTRACT	iv
ÖZET	vi
ACKNOWLEDGMENT	viii
CONTENTS	ix
LIST OF FIGURES	xii
LIST OF TABLES	xiv
PART 1	1
INTRODUCTION	1
PART 2	3
LITERATURE REVIEW	3
PART 3	5
THEORETICAL BACKGROUND	5
3.1. STAINLESS STEEL OVERVIEW	5
3.2. STAINLESS STEELS CLASSIFICATION	6
3.2.1. Austenitic Stainless Steel	7
3.2.2. Stainless Steel Type Ferritic	7
3.2.3. Stainless Steels Type Duplex	8
3.2.4. Stainless Steels Type Martensitic	9
3.2.5. Precipitation Hardening Stainless Steels	9
3.3. STEEL STRENGTH AND MECHANISMS	10
3.4. PROS AND CONS OF STAINLESS STEEL	11
3.5. APPLCATIONS OF STAINLESS STEEL	12
3.6. ALLOYING ELEMENTS	12
3.6.1. Chromium (Cr)	13
3.6.2. Molybdenum (Mo)	14
3.6.3. Manganese (Mn)	15
3.6.4. Nickel (Ni)	15
3.6.5. Carbon (C)	15
3.6.6. Nitrogen (N)	16

3.6.7. Niobium (Nb).....	17
3.6.8. Silicon (Si).....	17
3.6.9. Vanadium (V).....	18
3.6.10. Titanium (Ti).....	18
3.6.11. Aluminum (Al).....	18
3.7. MEDICAL IMPLANT CORROSION.....	19
3.7.1. Corrosion.....	19
3.7.2. Medical Implants Based Corrosion Types.....	20
3.7.2.2. Friction Corrosion.....	22
PART 4.....	25
POWDER METALLURGY.....	25
4.1. DEFINITION OF POWDER METALLURGY.....	25
4.2. METHODS OF POWDER PRODUCTION.....	26
4.3. ADVANTAGES AND DISADVANTAGES OF POWDER METALLURGY	27
4.4. CHARACTERIZATION IN MATERIALS.....	28
4.4.1. Powder Sampling.....	28
4.4.2. Particle Size Measurement.....	29
4.5. PRODUCTION SYSTEM.....	30
4.5.1. Mixing.....	30
4.5.2. Powder Compaction (Pressing).....	30
4.5.3. Isostatic Pressing.....	33
4.5.4. Powders Sintering.....	36
4.6. CHARACTERISTICS OF MATERIALS FABRICATED THROUGH POWDER METALLURGY TECHNIQUES.....	40
4.6.1. Mechanical Characteristics.....	40
4.6.2. Microstructural Features.....	41
4.6.3. Surface Related Properties.....	41
PART 5.....	43
METHODOLOGY.....	43
5.1. MATERIALS.....	43
5.2. MIXING.....	44
5.3. PRESSING.....	45

5.4. SINTERING	46
5.5. DENSITY MEASUREMENT	48
5.6. TENSILE TEST	48
5.7. HARDNESS TEST	49
5.8. OPTICAL MEASUREMENTS	50
5.9. CORROSION TEST	52
5.10. WEAR TEST	55
PART 6	57
RESULTS AND DISCUSSION	57
6.1. MICROSTRUCTURE	57
6.2. MECHANICAL PROPERTIES	61
6.3. CORROSION TEST RESULTS	64
6.4. WEAR TEST RESULTS	66
PART 7	67
CONCLUSION	67
REFERENCES.....	69
RESUME	77

LIST OF FIGURES

	<u>Page</u>
Figure 3.1. Correlations between the composition and properties of the stainless-steelgroup of alloys.....	13
Figure 3.2. Galvanic in sea water.....	21
Figure 3.3. Passivity in metals can be compromised through general corrosion, resulting in the degradation of the passive film, as well as through pitting corrosion.	24
Figure 4.1. Powder metallurgy stages.....	26
Figure 4.2. Methods of powder production.....	27
Figure 4.3. test procedure sieve analysis.....	29
Figure 4.4. Graphic diagrams of single-action die compaction and double-action die compaction	33
Figure 4.5. Cold isostatic pressing.	34
Figure 4.6. Hot way isostatic pressing.	35
Figure 4.7. Sintering process.....	38
Figure 5.1. The sequence of operations of this study.....	43
Figure 5.2. the RADWAG AS-60-220 C/2 weigh device.....	44
Figure 5.3. mixing TURBULA T2F device	45
Figure 5.4. Hydraulic pressing (Hidroliksan machine).....	46
Figure 5.5. Sintering device.	47
Figure 5.6. Produced samples after sintering.	47
Figure 5.7. The Radwag density kit.	48
Figure 5.8. SHIMADZU tensile test device.....	49
Figure 5.9. SHIMADZU hardness test device.	50
Figure 5.10. cold molding mold.....	51
Figure 5.11. grinding and polishing device.....	51
Figure 5.12. Nikon ECLIPSE L150 microscope.....	52
Figure 5.13. a) Soldering station device. b) Cold molding for corrosion samples. ...	52
Figure 5.14. Checking the conductivity of corrosion samples.....	53

	<u>Page</u>
Figure 5.15. prepared the (SBF) solution.....	54
Figure 5.16. a) Three-electrode electrochemical cell, b)Tafel corrosion set.	55
Figure 6.1. The optical micrographs of 316L	58
Figure 6.2. The optical micrographs of 316L+0.2Ti.....	59
Figure 6.3. The optical micrographs of 316L+0.5Ti.....	59
Figure 6.4. The optical micrographs of 316L+1Ti.....	60
Figure 6.5. The optical micrographs of 316L+0.2Zr	60
Figure 6.6. The optical micrographs of 316L+0.2Ti+0.2Zr.....	61
Figure 6.7 Microhardness of pm samples	64
Figure 6.8. Tafel curves of the alloys.....	65
Figure 6.9. Wear volume loss data of samples examined under 20N load	66

LIST OF TABLES

	<u>Page</u>
Table 3.1. Stainless steel properties.	6
Table 5.1. The sizes purities and density of the Powders.	43
Table 5.2 Chemical compositions of powder metal steels.	44
Table 5.3. Chemical composition of simulated body fluid (SBF).	53
Table 6.1. Mechanical properties of PM steel samples.....	63
Table 6.2. Ecorr, Icorr, and corrosion rate values of PM steel samples.....	65

SYMBOLS AND ABBREVIATIONS INDEX

SYMBOLS

Cr	: Chromium
Ni	: Nickel
Mo	: Molybdenum
V	: Vanadium
Mn	: Manganese
Fe	: Iron
Ti	: Titanium
Zr	: Zirconium
Al	: Aluminum
Nb	: Niobium
C	: Carbon
W	: Tungsten
Mg	: Magnesium
Co	: Cobalt
O	: Oxygen
N	: Nitrogen
Si	: Silicon

ABBREVIATIONS

PM	: Powder Metallurgy
----	---------------------

PART 1

INTRODUCTION

The recent surge in interest among academics in the area of material synthesis can be attributed to the growing need for high-performance materials in several industries. Titanium and stainless steel alloys are highly favored in various technical domains due to their biocompatibility, exceptional mechanical properties, and superior resistance to corrosion compared to other metallic materials [1]. Heat exchangers, reactor vessels, tanks, and turbine blades exemplify the broad use of titanium (Ti) in corrosion-resistant services, owing to its remarkable strength-to-weight ratio and extraordinary resistance to corrosion [2]. Despite the many potential uses of titanium, its high manufacturing costs are a consequence of the challenges associated with mining, melting, and machining the metal [3]. The use of powder metallurgy (PM) methods facilitates the production of near-net-shape components, thus enhancing the material consumption ratio and reducing the cost of machining [4].

Microalloyed steels, often enriched with elements like Molybdenum (Mo), Boron (B), and Vanadium (V), are frequently used in the construction industry due to their advantageous properties. These steels exhibit a low carbon content, enhancing their suitability for various building applications. The increase in strength results from several complex mechanisms, including dislocation strengthening, solid-solution strengthening, precipitation hardening, and grain refinement. Moreover, precipitation hardening has garnered significant attention from researchers [5]. By employing a variety of microalloying elements, contemporary microalloyed steels effectively acquire the desired properties. Titanium-vanadium (Ti-V) steels are a prime example of using titanium to enhance grain structure and vanadium to strengthen dispersion. These steels are commonly used in manipulating the microstructure during the hot rolling process, mainly due to their ability to significantly impede the recrystallization of austenite. Furthermore, the addition of vanadium enhances the dispersion, thereby

augmenting the overall strength of the steel[3,6] Aluminum, with a mass fraction exceeding 6%, is a key alloying element in titanium alloys, primarily due to its remarkable attributes of low density and significant solid solubility in titanium [7].

The weight proportion of titanium, vanadium, and aluminum in microalloyed steels typically does not exceed 0.20 percent. These steels belong to a category of materials that, through a diverse range of fortifying methods, demonstrate exceptional characteristics such as corrosion resistance, toughness, and commendable weldability [8].

Powder metallurgy (PM) technology will be used to add titanium (Ti) and zirconium (Zr) elemental powders to a 316 L stainless steel matrix. The powders will be added separately and together in set amounts (0.2, 0.5, and 1% by weight). According to ASTM E8M standards, the powders will be cold-pressed using one-way compression under 750 MPa. The microstructure, mechanical properties, tribological, and corrosion resistance of the PM steel samples will be investigated.

PART 2

LITERATURE REVIEW

Powder Metallurgy (PM) is recognized as an effective manufacturing process that enables the creation of intricate parts, including compact, functional, composite, and compatible structures, with high precision, exceptional strength, and minimal waste, according to experts. One of its major advantages is its cost-effectiveness. Essentially, powder metallurgy technology transforms various powders into engineered materials through a series of processes. Recently, a wide range of automotive parts have been mass-produced using powder metallurgical techniques.

The uniform distribution, affordability, and high quality of the outputs make powder metallurgy stand out as an innovative and novel manufacturing method. It also allows precise control over manufacturing temperatures and dissolution rates, enabling modification of the shapes and dimensions of the produced steels. By adjusting the sintering parameters, the desired ferrite and perlite structures can be achieved in the steel. Applications of powder metallurgy include jet engines, electrical connection components, high-temperature filters, armor-piercing materials, clock parts, orthopedic materials, and spare parts for automobiles and nuclear power plants [9].

Incorporating Nb-Al into micro-alloyed PM steel using precipitation hardening methods and microstructure refinement can increase the steel's strength. A significant improvement in strength is observed when precipitates such as NbC(N) and AlN are present because they inhibit grain growth during sintering [10].

Recently, flat products and tubes have accounted for a considerable portion of alloyed steel production, and there has been a notable increase in the production of alloyed steels intended for forging. Currently, micro-alloyed steels are being produced using the PM process, but the existing yield does not yet meet the required standards.

Several studies have highlighted the relationship between Nickel (Ni) and the mechanical properties, microstructure, and manufacturing of PM steel. The ideal nickel weight percentage for an alloy range between 1.5 and 2%, while the optimal sintering temperature for nickel used in everyday appliances is between 900 and 1000°C. The addition of nickel significantly affects the alloy's mechanical properties, as demonstrated in the cited research. Due to their high hardness, these samples have potential applications in areas such as corrosion-resistant marine equipment and shafts.

Erden et al. examined the efficiency of the alloying element Nb-Al in microalloy steel with respect to friction and wear. They found that adding Nb-Al powder, which constitutes 0.1-0.15-0.2% of the matrix weight, produces encouraging results. The wear resistance of the alloys with 2% Nb-Al was much higher than that of the unalloyed steel [10,11].

According to Erden, the enhanced mechanical properties are positively influenced by the addition of vanadium (V) and titanium (Ti). Vanadium can enhance titanium's grain refining capability and act as a dispersion strengthener in Ti-V microalloyed PM steels, increasing the hardenability of the metal [3].

Studies have shown that Zr exhibits extraordinary corrosion resistance when heated at 37°C in Hank's solution, opening up promising prospects for the biological applications of Ti-6Al-4V composite materials enhanced by microalloying [12].

H. A. Raghs et al. discovered that when corrosive wear fluid penetrates the wear zone, heat is dissipated from the wear environment, leading to more controlled abrasive wear behavior and an improvement in the surface quality of the material [13].

PART 3

THEORETICAL BACKGROUND

3.1. STAINLESS STEEL OVERVIEW

Chromium is renowned for its ability to enhance the heat resistance and corrosion resistance of iron [14]. It is a constituent in iron alloys, such as stainless steel, comprising at least 11.2% of the alloy composition [15]. Various steel compositions include elements like carbon (ranging from 0.03% to 1.1%), nitrogen, sulfur, aluminum, silicon, copper, nickel, selenium, niobium, and molybdenum. Certain types of stainless steels, for instance, the 340 series, are often identified by their AISI three-digit designations [16]. The presence of chromium in stainless steel imparts age-resistant properties to the alloy. It functions as a passive layer, protecting the underlying material from corrosion and facilitating self-repair in the absence of oxygen [17].

The techniques listed below can be used to increase corrosion resistance even more:

- 1) Incorporate not less than 8% nickel and increase the chromium concentration to at least 11.2%.
- 2) Involve molybdenum.
- 3) Additionally improving structural qualities and protecting against corrosion cracking is nitrogen injection.

Different applications require varying ratios of chromium and molybdenum, leading to the existence of several varieties of stainless steel. Stainless steel is ideally suited for tools that require the strength of steel combined with the ability to resist corrosion. This material is distinguished by its remarkable resistance to staining and corrosion, low maintenance needs, and notable sheen. Additionally, stainless steel can be bent, rolled, or shaped into a nearly limitless array of forms. Among its many applications, these versatile tools are particularly useful in surgical equipment. In the 1950s and

1960s, revolutionary scientific advancements made it feasible and desirable to produce a wide range of steel materials. Among the various types, austenitic stainless steel stands out as a popular choice [18]. Its defining features are its austenitic composition and face-centered cubic crystal structure. The addition of elements like nickel, manganese, and nitrogen during the steel melting process ensures the preservation of the austenitic microstructure across a wide temperature range, from very cold conditions to the softening point [19]. The uniform microstructure of austenitic stainless steels at room temperature means that their strength is not affected by heat treatment.

3.2. STAINLESS STEELS CLASSIFICATION

Stainless steels inherently contain a consistent amount of chromium, but their properties are often enhanced by the inclusion of additional alloying elements. A unique characteristic of stainless steels, setting them apart from other metals, is their classification based on microstructure, also known as crystalline structure. This structure refers to the arrangement of atoms within the steel's grains. Broadly, stainless steels can be classified into two primary types, characterized by the presence of chromium and chromium-nickel compounds in their chemical composition. Consequently, the microstructure is a key differentiating factor for several major groups of precipitation hardening materials, including duplex (austenitic-ferritic), martensitic, ferritic, and austenitic families. The mechanical properties of stainless steels, such as elongation, yield strength, elastic modulus, and ultimate tensile strength (UTS), are influenced by both the alloy chemistry and microstructure. This relationship is depicted in Table 3.1. An exceptional case is the 'Young's modulus,' which is significantly affected by the complex microstructure and chemical composition of the stainless-steel alloys [20].

Table 3.1. Stainless steel properties [21].

AISI stainless steel	Microstructure properties	Mechanical properties			Physical characteristics
		Elastic strength	Yield strength	Protraction – 50 mm%	
Austenitic	Austenite	480 -870	200-580	32-65	Non-heat able & non-magnets.
Ferritic	Ferrite	410-640	280-575	12-30	Magnets, non-heat able, & chloride-resistant.
Martensitic	Martensite	485-999	277-870	13-28	heat-treated, heat-enabled hardness
Duplex	Austenite & ferrite	688-910	409-912	15-45	High strength and heat-intolerant
Precipitation hard enable	Austenite & martensitic	890-995	271-992	10-32	high strength heat-treated hardening

3.2.1. Austenitic Stainless Steel

Austenitic stainless steel, comprising approximately 70% of the stainless steel produced industrially, is the most abundant and diverse category of stainless steels [22]. It is characterized by a stable austenitic phase with a face-centered cubic (FCC) crystal structure within its microstructure. Compared to other types of stainless steel, austenitic variants excel in areas such as corrosion resistance, non-magnetic properties, and weldability. One method to enhance their strength is through the use of cold metal forming processes [23]. The non-magnetic nature of austenite makes it particularly suitable for orthopedic implant materials, a desirable property given the widespread use of MRI [24]. An important consideration for orthopedic applications is the material's excellent resistance to corrosion in physiological fluids. Due to their inherent qualities, austenitic stainless steels are an excellent choice for orthopedic implants. However, they are more prone to pitting corrosion, stress corrosion cracking (SCC), and crevice corrosion compared to other types [25]. Additionally, they can be more vulnerable in harsh environments.

3.2.2. Stainless Steel Type Ferritic

Similar to carbon steels, ferritic stainless steels consistently display a ferrite microstructure characterized by a body-centered cubic (BCC) crystal structure. The chromium content in ferritic grades is typically maintained at a low level, around 0.08%, but can reach as high as 30.0%. While chromium is a predominant element, it's noteworthy that many ferritic phases may also contain trace amounts of nickel,

molybdenum (up to a concentration of about 4%), or sometimes none at all. Unlike austenitic stainless steels, many grades of ferritic stainless steels cannot be strengthened or hardened through heat treatment. Ferritic grades, which exhibit magnetic properties similar to carbon steel, are often used in applications where less toughness is required. However, it is important to note that ferritic stainless steels have a limited capacity to resist corrosion. They are particularly susceptible to stress corrosion cracking (SCC) when exposed to certain stressful conditions and corrosive environments [26]. Common applications of ferritic stainless steel include several automotive components such as bumpers and exhaust systems, as well as domestic appliances like water heaters [27].

3.2.3. Stainless Steels Type Duplex

The microstructure of duplex stainless steels (DSS) is a unique dual-phase composition of ferritic and austenitic structures, with both phases being stainless (i.e., containing more than 13% chromium) [28]. Commercial alloys often maintain a phase ratio close to 40/60, but ideally, a balanced blend of austenitic and ferritic phases is preferred. Duplex ferritic-austenitic steels amalgamate the advantageous features of both types, creating a distinct alloy. These materials offer greater resistance to wear and tear than purely ferritic steels, yet they do not match the strength of purely austenitic steels. While their resistance to stress corrosion cracking (SCC) may not be as robust as that of ferritic steels, it is still considerable.

Duplex stainless steels are characterized by magnetic properties and a significant inherent elastic limit. Notably, they exhibit a yield strength nearly double that of austenitic stainless steels, coupled with excellent corrosion resistance. Unlike austenitic stainless steel grades 304 and 316, their complex microstructure renders them highly resistant to various forms of corrosion, including chloride-induced stress corrosion [29]. Duplex stainless steels find applications in a range of fields, including heat exchangers, chemical processing, water filtration systems, marine environments, and paper production [27].

3.2.4. Stainless Steels Type Martensitic

Components made from martensitic stainless steels (MSS) exhibit exceptional mechanical properties, moderate corrosion resistance, and perform well under both high and low temperature conditions. These steels are versatile, finding applications in various industries, including turbines, pressure tanks, cutting tools, and offshore platforms for oil extraction. It is noteworthy that the properties of these steels can be effectively altered through heat treatment [30]. Martensitic stainless steels, a specific type of martensite, typically contain chromium (Cr) in the range of 11.5% to 18%, nickel (Ni) from 0.1% to 4.2%, and carbon (C) between 0.11% and 1.2%. These steels undergo significant property changes when subjected to heat. To prevent the formation of ferrite during cooling and to ensure a uniform transformation into a martensitic structure, martensitic stainless steels, with their complex composition, require comprehensive heat treatment [31]. Martensitic stainless steels comprise an alloy of carbon and chromium, forming a body-centered tetragonal (BCT) structure [32]. The strength of the alloy after heat treatment is dependent on its carbon content[33].

3.2.5. Precipitation Hardening Stainless Steels

Precipitation Hardening (PH) stainless steels are capable of achieving very high tensile strengths. These steels are primarily composed of chromium and nickel alloys. The key advantages of this particular group of stainless steel types [27] include ease of fabrication and exceptional corrosion resistance. Additionally, the material's strength is bolstered by its highly alloyed structure, which contains a relatively low mass proportion of carbon. Precipitation hardening [34] further enhances the strength of the crystalline phase. Compared to other martensitic types, PH stainless steels have superior strengthening capabilities, yet their corrosion resistance is comparable to that of austenitic steels [35].

Initially, the microstructure of precipitation-hardening stainless steels can exhibit characteristics of both austenitic and martensitic phases. Austenitic grades undergo heat treatment to transform into martensitic grades before precipitation hardening, a crucial step in the transformation process. This deliberate modification results in a

more durable product, improving its resilience and lifespan. Heating the martensitic structure leads to the formation of hard intermetallic compounds that precipitate from the crystal lattice, a process known as precipitation hardening.

Precipitation-hardening stainless steels are widely used in aerospace and technology sectors [27]. The most common grade in this category is 17-4 PH, also known as grade 630. As indicated in reference [35], this material consists of approximately 18% chromium, 5% nickel, 4.3% copper, and 0.33% niobium.

3.3. STEEL STRENGTH AND MECHANISMS

The mechanical properties of materials are influenced by thermal, mechanical, and chemical processes; however, it is the metallurgical structures that significantly determine these qualities. Strength is a crucial material property, impacting other characteristics such as resistance to plastic deformation. In metallic materials, plastic deformation is induced by the propagation of linear imperfections, known as dislocations. These dislocations often interact with other types of defects within the metal, influencing mechanical qualities like hardness, ductility, and strength. This phenomenon can be explained comprehensively through these mechanical properties.

Various processes contribute to the enhancement of material strength. These include deformation aging, precipitation hardening, grain size reduction, martensitic transformation, dispersion, cold working, and alloy hardening. To enhance the desirable characteristics of micro-alloyed steels, a thorough understanding of the complex relationship between mechanical properties and microstructure is required. Hardening techniques, which manipulate factors such as grain size, solidification process, precipitation, strain, and other microstructural aspects, can significantly improve the tensile strength of steels. The application of grain size reduction techniques in hardening processes results in improved toughness and longevity of the material.

3.4. PROS AND CONS OF STAINLESS STEEL

The numerous beneficial properties of stainless steel make it an ideal material for manufacturing a wide range of parts and components across various industrial sectors. Its extraordinary resistance to corrosion is primarily due to its high chromium content; steel with a chromium concentration of about 10.5% or more exhibits significantly greater corrosion resistance compared to steels without chromium. Customers benefit from stainless steel's excellent processability and ease of fabrication, low maintenance requirements, extended lifespan, aesthetically pleasing appearance, environmental sustainability, and recyclability. Additionally, its exceptional durability and resilience at both high and low temperatures further increase its suitability for diverse applications [36]. Once utilized, stainless steel typically does not require any additional treatments, coatings, or painting, adding to its practicality.

Austenitic stainless steels offer several benefits, chief among them being a high yield strength-to-tensile strength ratio, which is a result of their face-centered cubic (FCC) crystal structure. This structure also contributes to their excellent machinability. The strength of these steels can be further enhanced through cold working and a process known as progressive strain aging. One of the most notable properties of austenitic stainless steels is their exceptional corrosion resistance. Additionally, a distinctive feature of most austenitic stainless steels is their non-magnetic nature. This combination of properties makes them suitable for a wide range of applications, especially where corrosion resistance and non-magnetic characteristics are important.

316L stainless steel, even when utilized as an implant, is prone to specific types of corrosion, including pitting, stress corrosion cracking, and crevice corrosion [37,38]. Research indicates that when 316L corrodes in physiological environments, it releases elements such as iron, nickel, and chromium [39]. Nickel, which can be a hazardous substance when released into the environment, is present in 316L stainless steel in concentrations ranging from 11.0 to 16.0%. The release of nickel ions can pose health risks; they are known to be a common cause of contact dermatitis, the most prevalent type of contact allergy. Moreover, high concentrations of nickel in tissues could

potentially lead to cancer [40,41]. This underscores the importance of considering the biological compatibility of materials used in medical implants.

3.5. APPLICATIONS OF STAINLESS STEEL

Alloy steel, a valuable combination of metals, is used in the production of essential goods that are integral to our daily lives. This diverse group includes communication devices, steam boilers, automobiles, airplanes, dairy machinery, and equipment used in the leather, paper, and soap industries. It also extends to small household items, nuclear engineering, and machinery for producing exhaust systems.

Stainless steels, known for their corrosion resistance and durability, are commonly used in medical devices and food preservation equipment. In the medical field, these materials are utilized to manufacture items such as needles, screws, prosthetic limbs, scalpels, and even joint replacements like knee and hip caps. The remarkable ability of stainless-steel plates to preserve the natural qualities of food, including color and aroma, without any alteration, makes them highly sought after. They are widely used in various culinary applications, such as food and beverage containers, oven molds, and coated cooking pots.

3.6. ALLOYING ELEMENTS

The majority of metals aren't used in their pure form; instead, alloying components are added to change their properties for certain applications. An alloy can have some of its properties significantly changed by adding a specific quantity of a second element. The mechanical strength and corrosion resistance of unmixed iron are significantly enhanced by small quantities of other components, and it is not strong enough to be used as an active biomaterial. By incorporating chromium (Cr) into composites, it is possible to promote the formation of a protective layer known as a chromium oxide shield, or passive film [17]. The composition of stainless steels may include a variety of alloying elements, which can vary depending on the specific grade. Silicon (Si), chromium (Cr), nickel (Ni), molybdenum (Mo), titanium (Ti), niobium (Nb), and vanadium (V) are among the many secondary elements that can be found in these

alloys [27]. Figure 3.1 illustrates the complex interplay between the composition and properties of the stainless-steel group of alloys.

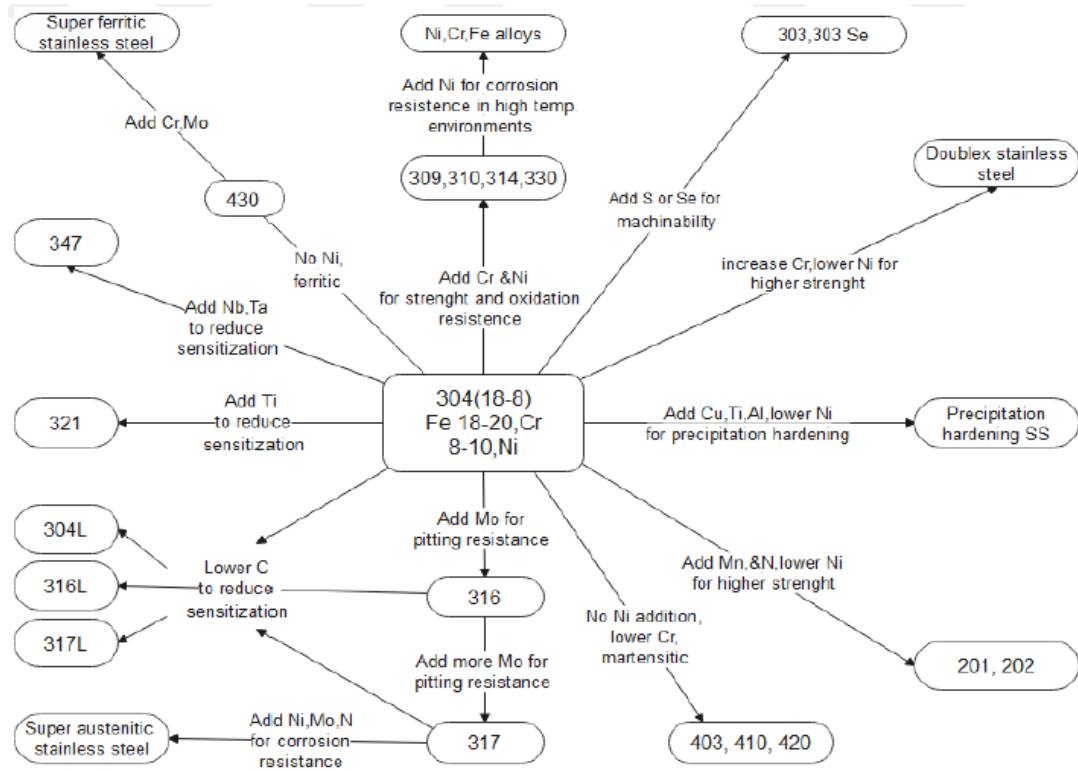


Figure 3.1. Correlations between the composition and properties of the stainless-steel group of alloys [16].

Figure 3.1 provides an in-depth discussion on the relationship between the chemical composition and the physical properties of stainless-steel alloys. This relationship is crucial as the specific elements present in the alloys, along with their concentrations, significantly influence the mechanical strength, corrosion resistance, thermal properties, and overall performance of stainless steel. Understanding this correlation is key in determining the suitability of various stainless-steel grades for different applications and environments.

3.6.1. Chromium (Cr)

Chromium is a vital element in stainless steel, especially for countering mild air corrosion. For effective corrosion resistance, the steel surface must maintain a consistent chromium passive layer, requiring a minimum chromium concentration of

about 10.5%. Increasing the chromium content in stainless steel directly enhances its level of corrosion resistance [42]. As a ferrite-forming element, chromium plays an essential role in maintaining the body-centered cubic structure of iron. To achieve an austenitic or duplex (austenitic-ferritic) structure with a high chromium content, additional nickel is required. Elevated concentrations of chromium also promote the formation of intermetallic phases.

In austenitic stainless steels, the typical chromium composition is about 18%, while second-generation duplex stainless steels may have a higher chromium concentration, around 22%. Chromium's ability to improve the oxidation resistance of materials at high temperatures is noteworthy. This aspect of chromium is particularly significant in controlling the complex processes involved in heat treatment and welding. These processes can lead to the formation and subsequent elimination of oxide scale and heat tint. When comparing duplex stainless steels to austenitic stainless steels, it is observed that duplex steels exhibit superior resistance in dissolving and eliminating heat tint.

3.6.2. Molybdenum (Mo)

Stainless steels exhibit significantly increased resistance to chloride-induced corrosion when molybdenum and chromium are combined. The addition of molybdenum in the presence of chlorides is three to four times more effective in enhancing corrosion resistance than chromium alone. Given that stainless steel typically contains about 18% chromium, incorporating molybdenum is an effective strategy to further reduce the risk of pitting and crevice corrosion [43]. However, it's important to note that molybdenum can also increase the tendency of stainless steels to form undesirable intermetallic phases, as it promotes ferrite formation. Consequently, in duplex stainless steels, the content of molybdenum is often limited to around 5%, and in austenitic stainless steels, it is usually kept below 7% to balance corrosion resistance with the stability of the alloy's microstructure.

3.6.3. Manganese (Mn)

Manganese is commonly added to stainless steels to enhance their malleability during the heating process. It plays a crucial role in stabilizing austenite, especially at lower temperatures. The effect of manganese on the equilibrium between ferrite and austenite is temperature-dependent; at higher temperatures, it contributes to the formation of austenite rather than ferrite. In duplex and austenitic stainless steels, manganese is particularly valuable as it enhances the solubility of nitrogen, allowing these steels to retain substantial amounts of this element. Additionally, due to its austenite-forming ability, manganese can partially replace nickel in stainless steel, contributing to the creation and stabilization of the austenitic phase.

3.6.4. Nickel (Ni)

The stabilizing effect of nickel on austenite within steel results in the contraction of the ferrite region and the expansion of the austenite region. Nickel maintains a remarkable resistance to oxidation and corrosion, even at very high temperatures. While nickel itself doesn't directly alter the grain size of steel, its addition can influence the steel's overall mechanical properties. Smaller grain sizes in steel, which can be achieved through various processing techniques, generally enhance hardness and strength. Moreover, nickel effectively inhibits the formation of scale on the material's surface. When combined with chromium, nickel enhances the steel's ductility, hardness, fatigue resistance, and critical cooling rate. In its elemental state, nickel exhibits a lower diffusion coefficient and a slower diffusion rate compared to several other elements [44].

3.6.5. Carbon (C)

Carbon, a nonmetallic element, is a component of all heat-resistant alloys, including stainless steel. It significantly enhances the strength of steel by efficiently stabilizing austenite. Carbon is a crucial alloying ingredient in austenitic, ferritic, and duplex stainless steels. However, when combined with other alloying elements, it tends to form carbides. To minimize the formation of chromium carbide (Cr_{23}C_6), controlled

cooling is often employed following high-temperature processes. This approach helps maintain a low carbon concentration in stainless steel, typically ranging from 0.003% to 0.038% in low carbon variants. The use of Cr23C6 aids in mitigating the reduction of chromium content, thereby preventing chromium depletion from the alloy solution. Carbon can induce defects in the lattice structure of microcrystals, potentially reducing their mechanical properties [22]. In martensitic stainless steels, carbon is intentionally introduced to achieve high levels of hardness and strength. It also enhances the creep resistance of austenitic stainless steels, improving their ability to withstand deformation under constant stress. High carbon steel is preferred for temporary surgical devices such as osteosynthesis plates and intramedullary nails due to its remarkable flexibility and stainless properties. However, it is generally removed after a few years due to its limited long-term corrosion resistance [45].

3.6.6. Nitrogen (N)

The introduction of nitrogen into austenitic and duplex stainless steels significantly improves their corrosion resistance and fracture toughness. Additionally, nitrogen increases the durability of these steels by augmenting their stress resistance [46]. In both austenitic and duplex stainless steels, the incorporation of nitrogen leads to enhanced mechanical strength and durability. Nitrogen's ability to inhibit the formation of intermetallic phases is particularly beneficial in the processing and manufacturing of duplex grades. It is added to these steels to reduce the likelihood of sigma phase formation, a detrimental phase that can occur in high chromium and molybdenum steels.

Furthermore, nitrogen serves as a viable alternative to nickel in austenitic stainless steels due to its exceptional ability to stabilize the austenitic phase. Achieving the desired phase equilibrium in duplex stainless steels often involves adjusting the nickel content and introducing nitrogen up to its maximum solubility limit. The presence of elements such as nickel and nitrogen, which promote austenite formation, combined with ferrite-forming elements like molybdenum and chromium, helps maintain a balanced duplex microstructure. This balanced interplay of austenite and ferrite-

forming elements is what gives duplex stainless steels their unique and advantageous properties.

3.6.7. Niobium (Nb)

Niobium is highly effective as an additive in preventing interfacial corrosion in certain types of stainless steels. The interest in niobium surged notably with the start of the space race in the 1950s, largely due to its exceptional qualities, including its ability to enhance the properties of metals it is alloyed with. The concept of a microalloy emerged from the improved characteristics observed in carbon steel containing a small amount of niobium. Niobium's primary application is as an alloying agent in microalloyed steels, where it significantly enhances the structural integrity of the metal.

A notable secondary application of niobium is in superalloys used in high-temperature components of aircraft engines. In addition, niobium contributes to increased wear resistance, especially in ferritic materials. It also plays a crucial role in applications requiring superconductivity, such as in Nb-Ti alloys, facilitating the development of innovative magnets. In stainless steels, niobium is typically used to stabilize the microstructure, especially in austenitic grades, by preventing the formation of harmful phases during heat treatment. The information enclosed in the tags provides confidence in the accuracy of these data regarding the uses and benefits of niobium[27].

3.6.8. Silicon (Si)

Steels with minimal amounts of silicon are known for their admirable hardenability, and this element also contributes to improved machinability [34]. Additionally, a small proportion of silicon can be added to Mo-treated austenitic stainless steels, enhancing their resistance to corrosion, particularly in sulfuric acid environments. Silicon also plays a crucial role in boosting the oxidation resistance of austenitic stainless steels and helps to prevent carburization at high temperatures. The accuracy and relevance of this information have been verified against reference [27].

3.6.9. Vanadium (V)

Vanadium, as a microalloying element, plays a significant role in enhancing the strength and wear resistance of microalloy steels through a process known as 'precipitation strengthening.' This process involves fortifying minute carbonitride particles that form during cooling or tempering, rather than solely improving hardenability [47]. Research has demonstrated that the addition of vanadium can augment the strength of steel while maintaining a consistent level of tensile strength. While some studies suggest that vanadium contributes to improved impact toughness, other research indicates that even small amounts of this element may have a negligible impact on steel's properties [48].

3.6.10. Titanium (Ti)

Titanium plays a crucial role as a stabilizing element in both ferritic and austenitic stainless steels. Additionally, it significantly enhances the steel's resistance to pitting corrosion. When titanium is incorporated into steel, it tends to form carbides. This propensity can lead to the presence of undissolved carbides within the steel's structure, potentially reducing its hardenability [27]. The addition of stabilizing elements like titanium to FeCr (Mo) and FeCrNi (Mo) alloys effectively reduces their susceptibility to intermetallic corrosion. Studies conducted in Hanks' solution reveal that 316L stainless steel alloyed with titanium exhibits greater corrosion resistance compared to the standard 316L variant.

3.6.11. Aluminum (Al)

Aluminum is added in significant quantities to certain types of steel to enhance their resistance to oxidation, serving a vital role in various heat-resistant classifications. The inclusion of aluminum in the precipitation hardening process of these steels plays a critical role in substantially improving their strength during the aging phase. This addition not only contributes to the material's durability at high temperatures but also reinforces its overall mechanical properties, making it more suitable for applications that require both heat resistance and structural integrity[49].

3.7. MEDICAL IMPLANT CORROSION

Corrosion remains a pervasive challenge for implants placed in the human body, often leading to implant failure. A key issue contributing to this failure is the release of non-biocompatible metal ions, commonly known as debris [50]. Medical implant corrosion is a significant concern; for instance, corrosion contributes to the failure of approximately 41% of Ti-6Al-4V and 316L implants. Understanding the corrosion behavior of different types of human body implants, particularly orthopedic implants, is crucial. This knowledge is vital for improving implant designs and material selection to enhance biocompatibility and longevity, thereby reducing the risk of implant failure due to corrosion [51].

3.7.1. Corrosion

Corrosion, characterized by the gradual deterioration of materials through electrochemical processes, presents a significant challenge for metallic medical devices exposed to the body's complex electrolytic environment. Metallic implants, in particular, are vulnerable to corrosion due to the composition of body fluids, which include water, salts, chlorine, plasma, amino acids, and mucous — components similar to those found in saliva [52]. The human body's aqueous solution contains various anions such as chloride, phosphate, and bicarbonate, along with cations like sodium (Na^+), potassium (K^+), calcium (Ca^{2+}), and magnesium (Mg^{2+}). This fluid also consists of both low molecular weight organic molecules and high molecular weight polymeric substances, and is saturated with dissolved oxygen [53].

Organic molecules within the body can disrupt the corrosion mechanisms of implants by absorbing byproducts of both anodic and cathodic reactions. Interactions between proteins and transition metals can potentially disrupt the electron-cation equilibrium on the implant surface, leading to metal displacement. Proteins that undergo surface digestion may also hinder oxygen transport in specific areas, thus causing localized corrosion. Additionally, bacteria can affect the corrosion-inhibiting properties of hydrogen produced in cathodic reactions by decomposing hydrogen near the implant. These factors often exacerbate corrosion.

The pH level, which typically averages around 7.0 in the human body, can vary from 3.2 to 9.5 due to different factors. Post-surgical conditions often see the pH level near the implant site ranging between 5.2 and 5.7. Clinical evidence suggests that implants can release metal ions due to corrosion, despite having oxide coatings intended for protection against such degradation. These observations underscore the complexity of corrosion phenomena in the physiological environment and the challenges in ensuring the longevity and safety of metallic implants.

3.7.2. Medical Implants Based Corrosion Types

Corrosion in metals can manifest in two primary forms: uniformly across the surface or localized to specific areas. Uniform corrosion typically results in an even degradation of the metal's surface. In contrast, localized corrosion occurs in specific, often small, areas of a metal surface. Medical implant metallic alloys are susceptible to a range of localized corrosion processes, such as galvanic, pitting, crevice, and fretting corrosion. These specific types of corrosion are collectively referred to as 'local corrosion'. Understanding the distinctions and characteristics of these corrosion types is crucial in the design and material selection for medical implants, to ensure their durability and biocompatibility in the challenging environment of the human body[54].

3.7.2.1. Corrosion of Galvanic

As shown in Figure 3.2, when exposed to harsh, corrosive environments, any inactive metal or alloy undergoes simultaneous oxidation and reduction reactions, leading to the establishment of an electrode potential, commonly referred to as E_{corr} (corrosion potential). The term 'galvanic corrosion' is used to describe the electrochemical potential difference that arises under these conditions. This type of corrosion occurs when two dissimilar metals, known as the anode and the cathode, are in contact within a chemical environment, leading to accelerated corrosion at the anode. The corrosion potentials of different metals and alloys, especially when exposed to seawater, have been experimentally observed and systematically arranged in what is known as the 'galvanic series.' This series helps in predicting and understanding the behavior of metal combinations in terms of their susceptibility to galvanic corrosion [55].

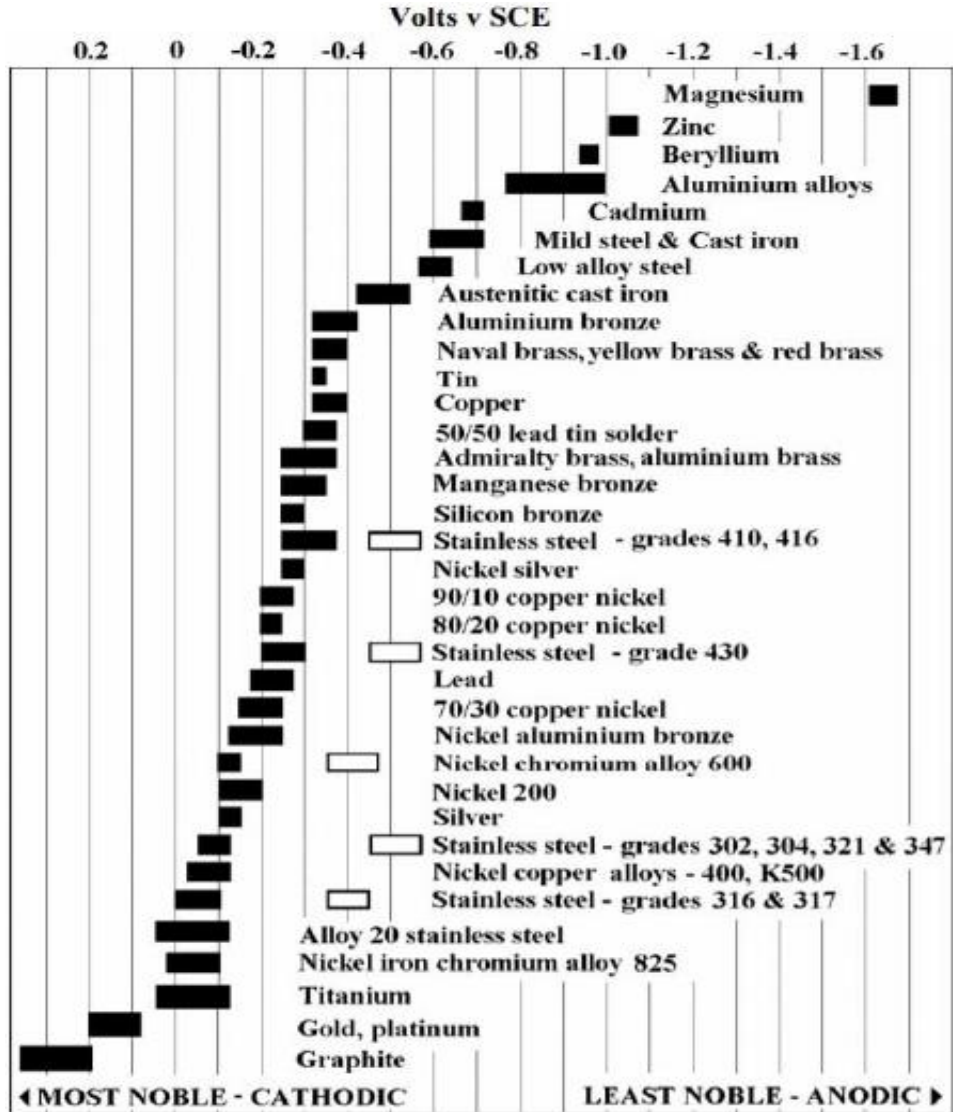


Figure 3.2. Galvanic in sea water [56].

The corrosion characteristics of metallic orthopedic implants used within the human body are often investigated using the galvanic series, which has been experimentally determined in pure seawater [56]. This approach is applicable because seawater shares similarities with diluted biological fluids and Simulated Body Fluids (SBF), such as Ringer's solution [57]. The electrode potential in these environments is influenced by various factors, including the specific type of pure element or metal, the composition of the electrolyte, the thickness of the oxide film layer on the metal, and the presence of different metals or alloys within the system [55]. The frequent use of diverse metals in orthopedic implants underscores the importance of understanding and addressing

the issue of galvanic corrosion, which can significantly impact the longevity and safety of these implants.

3.7.2.2. Friction Corrosion

Tribocorrosion, also referred to as friction corrosion, is a form of accelerated corrosion that occurs when surfaces are subjected to mechanical wear in addition to a corrosive environment. This phenomenon is commonly observed in medical implants where surfaces, such as bone plates and screw heads, are in constant contact and motion relative to each other. In these scenarios, even minor movements between contacting surfaces can initiate corrosion, especially in environments conducive to such reactions.

It's important to note that the presence of a corrosive liquid is not a prerequisite for tribocorrosion. Metal surfaces typically form a protective oxide layer when exposed to water or humidity, which helps in preventing corrosion. However, this oxide layer can be disrupted by micro-wear debris generated from friction between surfaces. This disruption alters the electrochemical equilibrium, potentially leading to renewed corrosion at the implant site. Such a pattern is often seen in orthopedic joints, like hip prostheses.

Factors contributing to tribocorrosion in implants include the presence of oxygen, proteins, wear debris, mechanical stresses applied to the implant, and the interaction with bone cells. The impact of these factors can vary in different parts of the body, influencing the distribution and severity of tribocorrosion in implants [58].

3.7.2.3. Crevice Corrosion

Crevice corrosion refers to a type of corrosion often associated with structural components, particularly in areas where external protection of a metal surface is inadequate. This form of corrosion manifests as fissures, which differ from fatigue fractures, and it typically occurs in regions with limited oxygen availability. An example is the flexible connections in a hip prosthesis, which represent a geometric

area vulnerable to crevice corrosion [59]. As material wears, microscopic galvanic cells form due to surface irregularities, leading to fractures.

In crevice corrosion, the oxygen level significantly drops both on the surface of the implant in contact with the electrolyte and within the crevice. While the outer metallic surface of the implant absorbs oxygen from the surrounding environment to maintain a stable O₂ level, the oxygen concentration inside the crevice decreases due to restricted circulation. Consequently, the metal within the crevice, experiencing lower oxygen levels, acts as an anode, and the metal outside functions as a cathode. This discrepancy in oxygen levels leads to a potential difference, initiating corrosion of the metal in the crevice [60].

Specific conditions, such as the presence of a narrow and deep crevice, the interconnection between implant components (like a plate and screw head), or the presence of flaws like fatigue fractures, can facilitate this process. Compared to other metallic implant materials, Type 316L stainless steel is notably more susceptible to crevice corrosion attack [61]. A common instance is the corrosion of screw heads in stainless steel bone plates that contact countersink holes. Although failures induced by crevice corrosion are rare, crack propagation in the countersink area of bone plates is a potential risk. Addressing crevice corrosion effectively involves thoughtful device design and material selection.

3.7.2.4. Pitting Corrosion

Pitting is a severe form of localized corrosion that leads to significant material degradation and substantial release of metal ions. This type of corrosion is characterized by the formation of small cavities or pits on the surface of a material, typically covered by a thin, resilient, self-repairing passive layer. It is believed that these pits form due to the interaction between harmful ions and the passive film at vulnerable or defective spots. While pits can sometimes be easily detected, they often remain hidden, posing a significant risk of stress corrosion cracking (SCC) or fatigue cracks. Such hidden flaws can lead to catastrophic failures in practical applications [62].

The development of pitting is largely influenced by the formation of a surface layer or coating that induces a state of passivity in the material, effectively preventing surface deterioration and corrosion. Pitting occurs when localized anodic activity breaks through the passive film. This can be triggered by breaches in the film, surface irregularities due to changes in scaling layers, inadequate protection, or localized accumulation of metals, among other factors. The cathodic area may be situated outside the pit. Near the bottom of the pits, the corrosion current density is typically higher. A protective layer over the pit's surface [63] hinders the upward migration of metal ions or other elements. As oxygen depletion progresses, the electrochemical potential between the surrounding metal and the pit changes. Figure 3.3 illustrates the breakdown of passivity and the complex process of pitting attack. Once a pit forms, metal ions often precipitate, creating a protective coating that covers the pit. This coating acts as a passivate, blocking the entry of oxygen and solutions into the pit, potentially restoring the protective barrier [64].

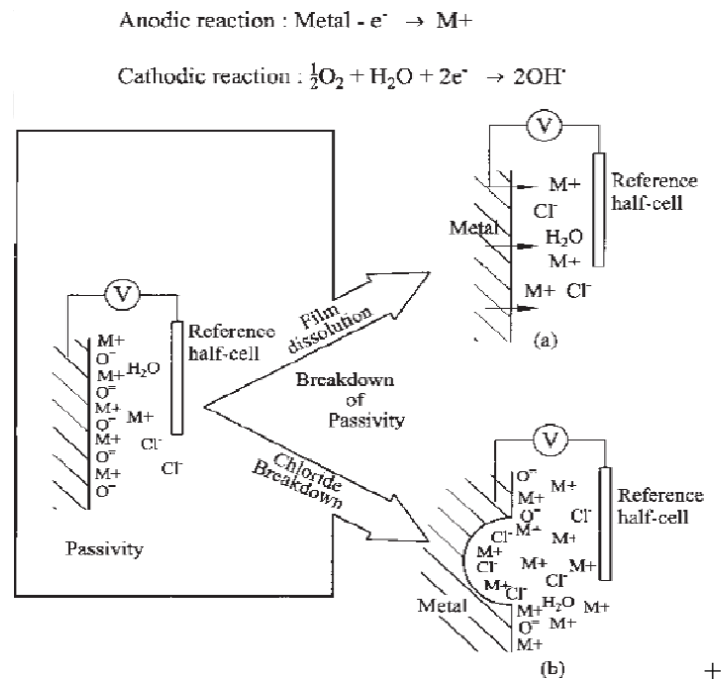


Figure 3.3. Passivity in metals can be compromised through general corrosion, resulting in the degradation of the passive film, as well as through pitting corrosion [64].

PART 4

POWDER METALLURGY

4.1. DEFINITION OF POWDER METALLURGY

The process of manufacturing metal components using powder metallurgy (PM) involves controlled heating of metal powders while keeping the temperatures below the melting points of the individual powders. Powder metallurgy, often referred to as PM, is a method for producing metal parts that are nearly finished. It involves the precise mixing of unalloyed or alloyed powders in predetermined proportions. After proper mixing, the powders are compressed using a suitable mold and heated to a specified sintering temperature to achieve the desired metallurgical properties. This process allows for precise control over the mechanical, chemical, and physical properties of homogeneous materials [65].

The process of powder metallurgy involves several key steps:

- 1) **Generation of Powder:** The process begins with the creation of a powdered substance or a mixture of powders that contains the necessary constituents in the required proportions.
- 2) **Mixing and Blending:** The powders undergo thorough mixing and blending to achieve the desired characteristics and properties.
- 3) **Shaping:** The powders are formed and manipulated into the desired shapes and dimensions while reinforcing the sections.
- 4) **Sintering:** The compacts formed from the powders are subjected to high temperatures during sintering, which enhances their strength.
- 5) These steps are essential in the production of metal parts using powder metallurgy, allowing for precise control over the final product's properties and performance.

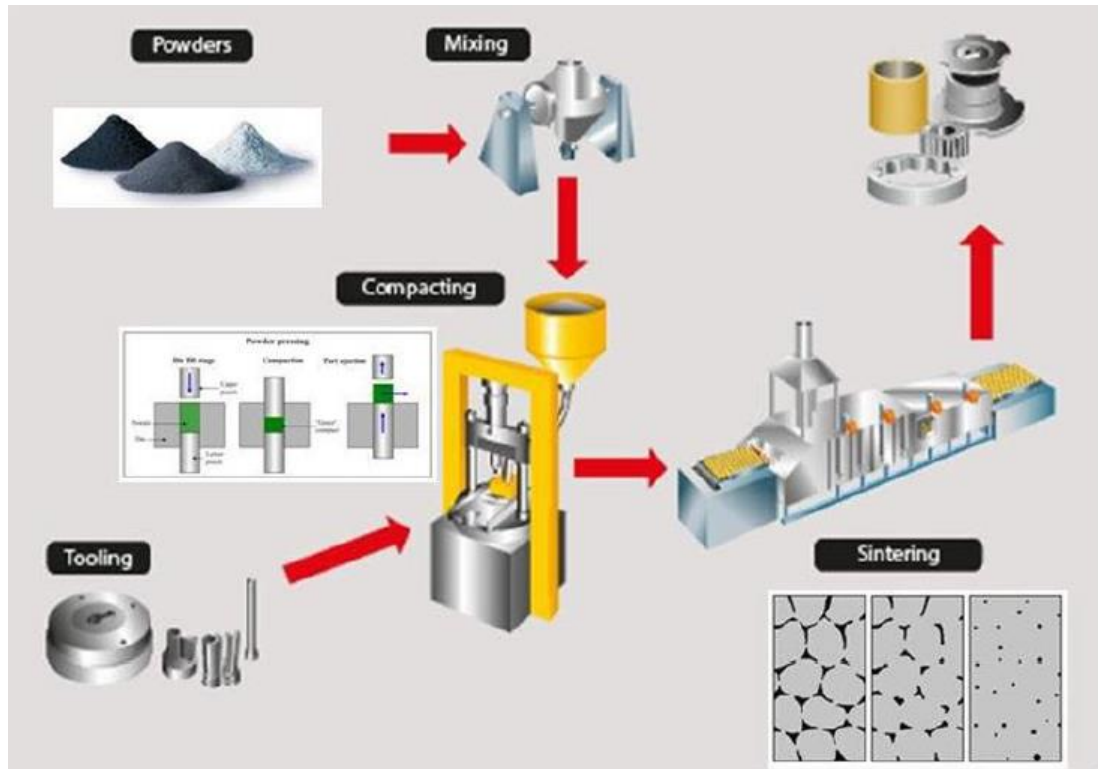


Figure 4.1. Powder metallurgy stages [66].

4.2. METHODS OF POWDER PRODUCTION

Metallic powders can be produced through three methods: atomization, chemical reduction, and electrolytic deposition. Atomization breaks down molten metal into fine droplets, which solidify into powder particles. Chemical reduction converts metal ions into solid particles, while electrolytic deposition deposits metal powders onto a substrate. Each method offers unique advantages and applications, as illustrated in Figure 4.2. Each method has its own advantages and applications.

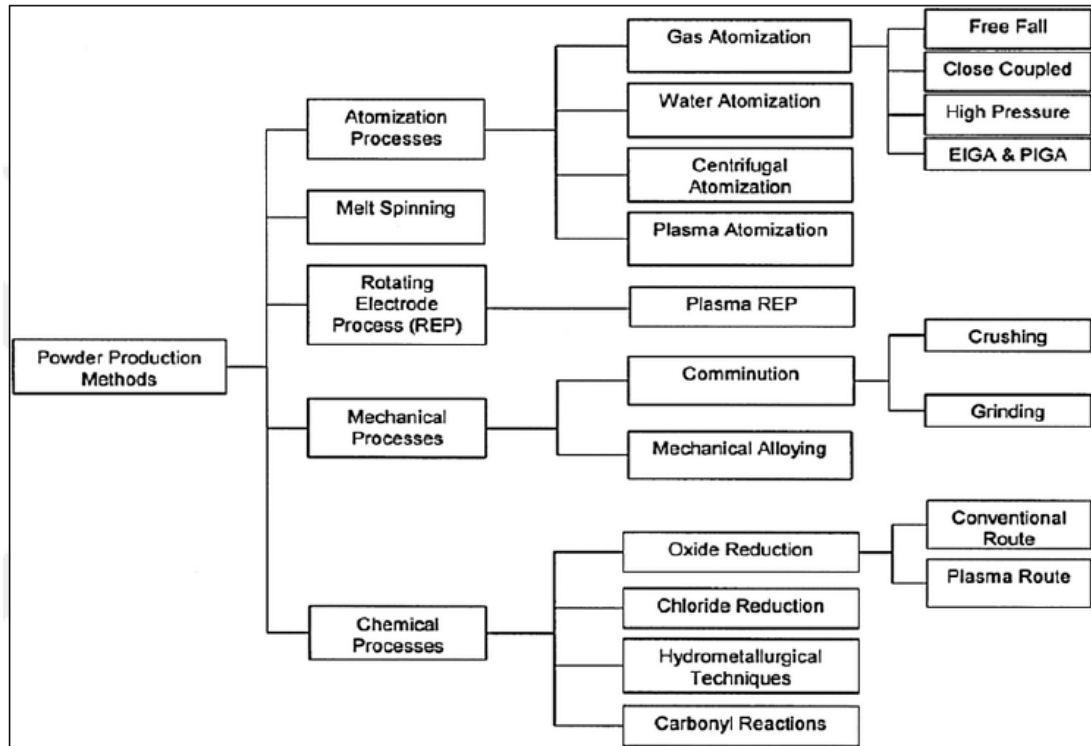


Figure 4.2. Methods of powder production [67].

4.3. ADVANTAGES AND DISADVANTAGES OF POWDER METALLURGY

The advantages can be listed as follows:

- Parts produced in powder metallurgy can be manufactured in final shape or close to their final shape.
- Parts that are not easy to machine with various other manufacturing methods can be formed using T/M.
- Since production work is carried out using molds, labor and time can be saved in production.
- Since enough powder is used in the molds in production, material savings can be made compared to machining.
- Exactness in dimensions can be ensured during production. The reason for this is that expansion does not occur in powder metallurgy, as in other casting processes performed with molds.
- Some alloys produced using T/M cannot be produced by other methods.
- It is better than other production methods in terms of shape and size control.

- The corrosion and wear resistance of parts produced with powder metallurgy is at good levels.
- Since the powders are blended in the desired composition, it is easy to produce materials with various properties.
- In this method, it is possible to produce porous samples by leaving the desired space between the powder particles for the production of porous metal parts.
- Since scrap parts are generally used to produce powder in the T/M method, the production cost decreases in this method.
- Powder metallurgy method is an economical and automatable method for mass production.

The disadvantages can be listed as follows:

- In the powder metallurgy method, the wear levels of the molds used in production must be high. This is because metal powders have corrosive properties. This desired feature in the molds increases the cost in production.
- Metal powders are expensive and metal powder production is difficult.
- The cost of the powders and other materials used can be high.
- The strength of metal materials is low because the bonds they contain are not strong.
- Metal powders are difficult to transport and store, care must be taken.
- Changes in density that may occur in the part during production can sometimes be a disadvantage [68].

4.4. CHARACTERIZATION IN MATERIALS

4.4.1. Powder Sampling

There are a few methods you might employ to finish the difficult and drawn-out process of powder sampling. It is common practice to take small samples from various areas, combine them, and apply them. The particles have a coherent overall shape, and due to the conditions, there is a high likelihood that they will stick together. Particle aggregation is a possible eventuality. Surface moisture might lead to excessive aggregation. Clinging agglomerates are particles that are attached to weak forces and

can be destroyed by small shear pressures. The majority of the time, mechanical and ultrasonic agitation methods have an impact on the particle dispersion and subsequent measurement of their characteristics. Typically, mechanical mixing or ultrasonic agitation are used to spread the flocculation formation [69].

4.4.2. Particle Size Measurement

Particle size and shape characterization are crucial in various industries, but assessing these properties becomes more complex when particles deviate from perfect spherical shapes. Factors like particle geometry and characteristic diameter are important considerations. Several methods can be employed to determine particle size, including direct imaging techniques, sieve analysis, dynamic light scattering, and laser diffraction. Sieve analysis is a well-established technique for characterizing particle size distributions, separating particles into different size fractions. There are two primary approaches: dry sieving for particles between 30 μm and 125 mm, and wet sieving for particles between 20 μm and 3 mm. By carefully measuring and quantifying the mass fraction of particles in each sieve, a cumulative distribution of particle sizes can be obtained [70,71].

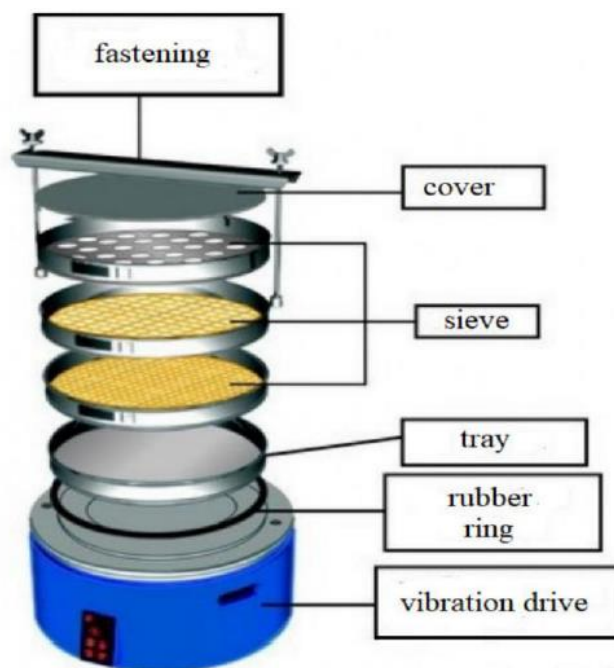


Figure 4.3. test procedure sieve analysis [72].

4.5. PRODUCTION SYSTEM

4.5.1. Mixing

Powder metallurgy relies on combining powders that require extensive mixing before compaction to ensure consistency and improve the final product. If you want better pressing and sintering results and a more uniform distribution of particle sizes, mixing is the way to go [73]. Several variables affect the mixing and blending process. These include the physical properties of the powders, the size of the mixer, the mixing and rotational speeds, the quantity of powder in the mixer, the duration of the mixing process, and the humidity and weather conditions. Mechanical and physio-chemical methods may be used to create powders. Metal powders may exhibit a wide range of properties depending on the production procedures. Before commencing the pressing process, precise amounts of powder can be added to the mixing mills or measured using precision scales. The quality of metal powders determines how effective production processes are, and the cost component of manufacturing is crucial.

4.5.2. Powder Compaction (Pressing)

Ensuring complete filling of the mold with metal powders is crucial in manufacturing using molds. Cold pressing the powders in the mold is assumed to align their theoretical densities closely with the actual densities. Uniform and consistent pressing force compresses the metal powder to a density dependent on the material's theoretical density. Key factors include the powder particles' shape, dimensions, surface area, composition, and any prior treatment [74].

Typically, pressing is done at room temperature using precision-engineered steel molds. Cemented carbide-based, heat-hardened tool steel is essential in mold-making. The number of cavities changes in size and position in direct response to increasing compressive force and pressure ratio. Higher pressure enhances powder particle contact and increases the powder's surface area. Density inversely correlates with pore quantity, and tensile strength in powder metallurgy components varies with material porosity. There is a positive correlation between tensile strength ratio and density ratio.

At first glance, powder compression seems simple but involves several aspects. Initially, friction inside the mold exerts significant stress, reducing towards the center. Energy generation decreases due to friction between the powder and mold surface, and interparticle friction. Measuring the resistance during product removal, depending on the friction inside the mold and the product, is crucial. Effective lubrication is vital for successful forming and demolding without hindering the sintering process [75].

Mold oscillation compacts the introduced powders, enhancing density. Density under vibration depends on the particles' dispersion pattern and structure. Powders with irregular shapes see a more significant increase compared to flat, spherical ones, due to their lower relative densities and higher density ratios in spherical shapes. Relative density is calculated by comparing estimated and raw density.

Cold pressing and hot pressing are two main pressing techniques in the industry. Hot pressing applies pressure and heat simultaneously, while cold pressing introduces heat after pressing. Cold or hot isostatic pressing methods, compared to using rigid molds, can achieve better mechanical properties and precision. Pressing techniques ensure even pressure distribution on powder masses, achieving higher wet density and strength even at low pressures. Materials produced using hot isostatic pressing show significant mechanical properties, including tensile and fatigue strength. Cold isostatic pressing and hot isostatic pressing are elaborated in the following categories [76].

4.5.2.1. Single Action Die Compaction

In traditional powder compression processes, uniaxial compression is commonly employed. As soon as the powder mixture is introduced into the mold, the top pressure plate begins the compression. Utilizing the bottom piston facilitates the easy removal of the final product from the mold. To expedite the extraction of components, lubricant is applied to the mold walls, aiding in the compression process. During single action compaction, as the material is compressed, its density increases, typically leading to a rise in the applied pressure. This increase in density might be attributed to a reduction in the number of voids in the powders used, resulting in a decrease in volume while

maintaining constant mass. Although this method is useful in certain applications, it is not ideal for producing metal components with high length-to-width ratios and complex designs, as it may not achieve the necessary density.

4.5.2.2. Double Action Die Compaction

Punches in compression processes possess a significant amount of energy. The impact intensity of a punch can vary, depending on whether its trajectory is uniform or variable. The distribution of raw density in the powder exhibits considerable variability, influenced by factors such as the frictional forces generated by the powder, punches, particles, and mold surface. To address these issues, some practitioners use lubricants to reduce friction or employ specific compression techniques to mitigate these effects.

Achieving complete density using the single action compaction method is challenging. However, the double action compaction method, where the powder is compressed by both upper and lower punches, increases friction between the powder particles and the mold wall, overcoming the spring force of the material. This technique allows the mold to apply consistent pressure on the powder with both punches as they descend to the lowest position. After compression, the component is ejected from the mold by the upward movement of the bottom punch. This results in a more uniform density distribution compared to components produced by single action compaction. Typically, the lowest density value is found in the central part of the compacted area, following a symmetrical distribution pattern [77].

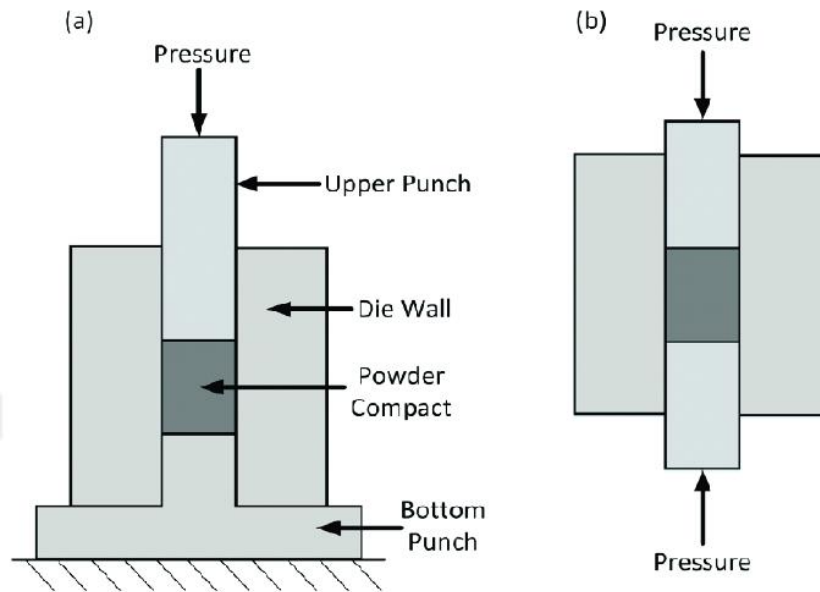


Figure 4.4. Graphic diagrams of single-action die compaction and double-action die compaction [78].

4.5.3. Isostatic Pressing

One well-established technique is isostatic pressing, sometimes referred to as hydraulic pressing of metal particles. In this method, compressible powder particles are placed in a mold made of flexible, hermetically sealed material. Then, a tremendous amount of intense pressure is uniformly applied to the entire mold. Products manufactured through isostatic pressing exhibit consistent density across all three dimensions (diameter, length, and height). A uniform and consistent density distribution is achieved by applying force evenly to all surfaces and by reducing friction against the mold wall. This method is particularly practical and essential for creating objects with complex shapes. Isostatic pressing, whether performed hot or cold, has varied applications, as noted in reference [79].

4.5.3.1. Cold Way Isostatic Pressing

Cold isostatic pressing derives from the technique of applying pressure at ambient temperature using cold water or oil. As depicted in Figure 4.5, in the oil-prepared pressing section, powders undergo the cold isostatic pressing technique inside a rubber mold, leading to their compression. Incorporating oil into the mold ensures a uniform

pressure distribution across the entire sample when force is applied with the pressure piston. While compression pressures can exceed 1400 MPa, it is more common to utilize pressures below 350 MPa in this process. The use of elastomers, polyvinyl chloride, or rubber as materials for casting molds in the cold isostatic process is widely recognized and practiced. Flexible molds are particularly advantageous for fabricating products with complex shapes. Moreover, employing rubber substantially reduces mold costs. As detailed in reference , this pressing technique is applied in the production of various objects, including tool steel billets and superalloy aircraft turbines[80].

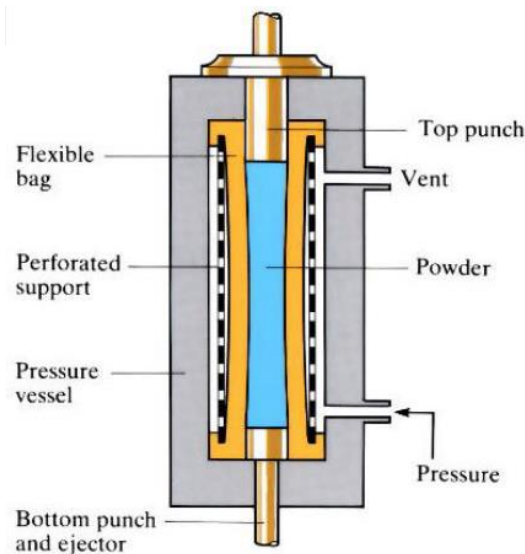


Figure 4.5. Cold isostatic pressing [80].

4.5.3.2. Hot Way Isostatic Pressing

Pressure is applied to the statically or dynamically heated powder along a single axis from one or more locations in opposing directions. Pressing hot metal into a compressed box is one of the most traditional ways of compacting powder metal. Refer to Figure 4.8. Although hot pressing yields products with superior qualities, there are several disadvantages. The variables impacting the pressing process include the gap between the box walls and the moving bushings, gradual wear and tear of tools and dies, loss of samples, and heat conduction from the punch surfaces to the die walls, leading to deterioration of the compressed surfaces, as outlined in reference [81].

When compared with traditional cold pressing methods, several advantages of hot pressing become evident. The first benefit is the increased efficiency due to lower energy consumption in hot pressing. Secondly, hot pressing significantly reduces processing time compared to conventional cold pressing techniques. Moreover, hot pressing at lower temperatures offers numerous benefits. The results indicate that hot pressing is faster and more effective than traditional cold pressing methods, achieving higher densities than those attainable by cold pressing. Hot pressing, a highly efficient process for consolidating molten metal, encompasses a variety of approaches. The selection of a specific method depends on the inherent physical properties of the metals. However, common elements across all hot pressing procedures include metallurgical bonding, corrosion resistance, surface quality, density (approaching theoretical density), and mechanical properties, making products produced by the hot isostatic pressing technique particularly advantageous in the aviation industry, as discussed in reference [82].

Unlike the cold isostatic pressing method, which uses a liquid to compress powder particles within a chamber, the hot isostatic pressing method employs an inert gas, such as argon. This alternative method offers distinct advantages. By applying pressures between 150 and 350 MPa, it successfully raises the temperature parameter to an impressive 1700°C.

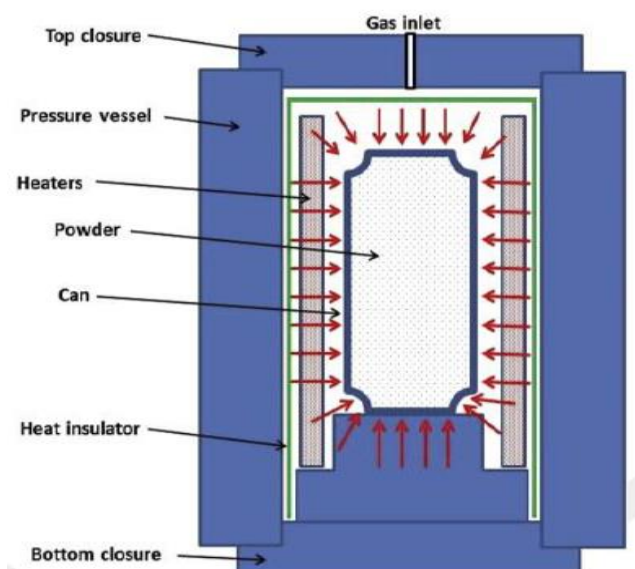


Figure 4.6. Hot way isostatic pressing [83].

4.5.4. Powders Sintering

Sintering refers to a highly controlled, high-temperature process that enhances the strength of powder particles. It transforms the initial mechanical bonds, formed when particles are compressed and shaped in the mold, into strong metallic linkages, thus improving product strength. The strength ratio of the component undergoes significant alteration before and during the sintering process. In single-component systems, sintering occurs at a temperature above the melting point of the component with the lowest melting point. However, in multi-component systems, it typically takes place at a temperature above the metal's absolute melting point. Sintering can increase the melting points of some refractory materials by up to 90%, usually by heating the material to 70% to 80% of its original melting point [84].

Sintering is a thermal process that causes material transport, altering the volume and arrangement of pores within powders. It results in a reduced overall surface area and an increased number of contact points. A sintering furnace, or apparatus, controls the temperature and duration of the process. Additionally, it aids in environmental conservation by removing binders and lubricants, and allows for post-sintering heat treatment of the component if necessary. After compression, spherical powder particles are closely positioned, as illustrated in Figure 4.7. This proximity leads to the formation of welds, which are then strengthened during sintering. Initially, particles increase in size, reducing the pore size, and eventually, pore channels transform into closed pores.

The sintering process reduces the high surface energy of powder particles, achieving the desired size and eliminating porosity within the internal structure. The ease of fusion of small powder particles is inversely related to their surface energy and directly related to their volume ratio and diameter. In ceramics, sintering increases transparency, heat conductivity, density, and strength; in polymers, it enhances density and strength; and in metals, it significantly boosts strength and conductivity. Materials similar to porous bronzes, such as sintered alloys, are formed at temperatures between 600 and 800 degrees Celsius, iron-group metal alloys at 1000 to 1300 degrees Celsius, and hard alloys at 1400 to 1600 degrees Celsius. Sintering duration and temperature

vary depending on the material type. Hard alloy materials typically require over an hour of sintering, while diamond alloys can be processed in about 30 minutes. There is an inverse relationship between temperature and sintering time: higher temperatures accelerate sintering, while lower temperatures necessitate longer periods [85]. Increased sintering temperature improves ductility, density, electrical conductivity, and strength.

In the initial stages of sintering, powder particles are in close proximity. The process comprises three distinct stages, each optimizing the material's reactive power potential by minimizing internal energy. This reduction results from factors like decreased surface area due to increased particle contact, reduction in pore volume or sphericalization, and elimination of solid-liquid phase disparities in multi-component systems [86]. During sintering, microstructural changes occur due to temperature-dependent atomic transport orientations, including dimensional alterations, pore size and shape adjustments, and grit formation. Atomic transport can occur via surface diffusion, volume diffusion, along grain boundaries, through plastic flow, condensation, and evaporation. Surface diffusion does not change dimensions. Sintering involves a multitude of variables.

The sintering process involves two distinct atmospheric conditions: reducing atmospheres and oxidizing atmospheres. Reducing atmospheres, which are employed to prevent oxidation of the material, typically consist of gases like hydrogen (H) and methane (CH₄). These environments facilitate the removal of oxides from the metal surfaces, enabling better sintering. On the other hand, oxidizing atmospheres are used when the process requires controlled oxidation. These atmospheres may include gases such as carbon dioxide (CO₂) and water vapor (H₂O). Additionally, nitride atmospheres, which are primarily composed of ammonia gas (NH₃), create gaseous environments conducive to the formation of nitrides on the material's surface. Each type of atmosphere is chosen based on the desired properties of the final product and the characteristics of the materials being sintered.

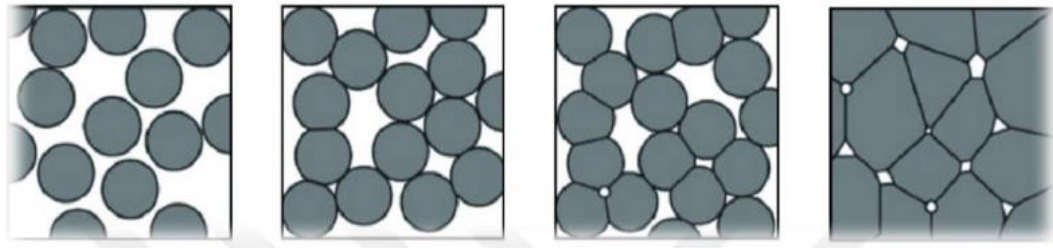


Figure 4.7. Sintering process [87].

4.5.4.1. Sintering of Liquid Phase

During the sintering process, metal powder particles undergo transformation instead of melting when exposed to temperatures below their melting point. Utilizing a combination of powders in the sintering process proves advantageous, allowing the procedure to be executed at a temperature below the fusion point of the mixture's constituents. Typically, materials are not subjected to sintering temperatures exceeding their low melting points. This method, as mentioned in reference [88], is known as liquid phase sintering.

Throughout the sintering process, a coherent mass of powdered particles forms along with a liquid phase. Liquid phase sintering accelerates both the initiation of particle aggregation and the overall sintering rate [89]. Capillary forces generated by the liquid phase draw the powder particles together, facilitating a self-sustaining condensation process independent of external pressure. Subsequently, a fluid phase allows for reorganization by reducing inter-particle friction. This results in noticeable changes in the pore structure and component characteristics, including antiparticle bonding, ductility, and strength, conductivity, and corrosion resistance.

A significant advancement in sintering techniques is the use of solid state-controlled sintering, which shows notable improvements over traditional liquid stage sintering methods. In this stage, the condensation process slows down due to the formation of a skeletal framework [90]. Typically, sintering compacts involve using single-phase particle structures within a temperature range of about 80% of the material's melting point. Indicators of changes during sintering include dimensional shifts and microstructural alterations, which are telltale signs of transformations in the

component's mechanical and physical properties. Decreased strength can be attributed to changes in the raw materials' microstructure.

In the first stage of sintering, there is a significant increase in the contact area between powder particles, leading to a notable reduction in the distance between their axes and the smoothing out of pre-existing pores. This leads to a reduction in the component's size and an increase in density. The particles gradually coalesce in the subsequent phase. Over time, pores naturally develop and diminish in size as materials move through the framework. Grain growth is observed as a final stage [91].

4.5.4.2. Sintering of Solid State

Solid-state sintering refers to the transformative process occurring when a single-element mixture is subjected to sintering. This process results in changes in the mixture's dimensions, morphology, and its mechanical and physical properties. Reactive power aids the sintering process by reducing the system's free energy. Consequently, there is an observed increase in dust and grain accumulation, along with a reduction in the total surface area of the grain boundaries. The intensification of these boundaries becomes more pronounced as their degree of curvature increases. Atomic and boundary movements are primarily governed by temperature, with a significant exponential increase in atomic emission as temperature rises. Due to the dynamic movement in the grain boundary area, the formation of larger grains occurs while smaller particles gradually diminish. The solid-state sintering process is driven by the mobility of materials and the dispersion of grains. Conducting sintering at elevated temperatures is advantageous due to the increased propensity for material diffusion. The material's structural integrity remains intact during the sintering process. The inclusion of a solid phase within a material facilitates two intrinsic phenomena: diffusion and density augmentation. The difference in free energy between the surface and neck regions of the grain provides the essential impetus for the process of solid-state sintering within the material's internal framework. The process begins with point contact between grains, leading to grain displacement and increased inter-grain interaction. Over time, the contacting particles develop necks, also known as sintering bridges. Despite their proximity, there remains a distinct separation between the dust

particles in this area. As the first stage nears completion, the particle centers with neck development gradually draw closer, leading to the formation of volumetrically shrunken grains [92].

The intermediate stage of sintering is characterized by the growth of inter-particle necks and the reshaping of particles beyond a certain neck width threshold. Both inter- and intra-particle spaces reduce during this stage. As void ratios decrease, the material undergoes physiological contraction. Grain formation occurs as particles aggregate towards the end of the intermediate stage [93].

4.6. CHARACTERISTICS OF MATERIALS FABRICATED THROUGH POWDER METALLURGY TECHNIQUES

4.6.1. Mechanical Characteristics

When a single element is sintered into a mixture, the solid-state sintering process alters the mechanical and physical properties of the component, as well as its dimensions. A critical aspect of sintering is reactive power, which reduces the system's available energy. The rise in dust and grains, coupled with a decrease in the total grain boundary area, can be attributed to free energy dissipation. There's an acceleration in grain boundaries alongside an increase in curvature radii. Temperature predominantly governs the mobility of atoms and boundaries, with the rate of atomic emission rising sharply as temperature increases. This dynamic movement in the grain boundary area leads to the formation of larger grains while smaller particles disappear simultaneously. The solid-state sintering process is driven by material displacement and grain diffusion. Heating the material to high temperatures is one of the most effective methods to ensure consistent diffusion during sintering. It is crucial to note that the material's internal structure remains unchanged post-sintering. The presence of a solid phase within the material facilitates two inherent processes: diffusion and an increase in density. Considering the free energy difference between the grain surface and neck areas is essential to understanding the consolidation process within the material's internal structure. The process of solid-state sintering initiates when grains

come into close proximity. The first stage is marked by grain mobility, followed by a second phase where increased and more pronounced reciprocal contact occurs.

Over time, particles in close proximity often develop sintering bridges or necks. Despite their proximity, dust particles in this area maintain their distinct spatial arrangement. At the end of the first stage, particle centers progressively move closer due to neck formation, resulting in compressed grains with reduced volume.

During the intermediate sintering process, the gaps between particles become noticeably larger. Particle shape changes only occur if the neck width exceeds a certain threshold. There is a discernible reduction both within and between particles. As void ratios decrease, the material's physical structure contracts. Grain development takes place at the culmination of the intermediate stage.

4.6.2. Microstructural Features

The microstructure of a material is defined by its geometric configuration, the arrangement of its constituent elements, and the chemical and structural characteristics of these components. This microstructure encompasses various flaws and phases that constitute the material. Significantly, a material's microstructure profoundly influences its properties. Understanding the unique aspects of a material's microstructure, as well as how various factors relate to it, is crucial when determining how to utilize the ore. In the field of materials science, establishing these connections involves one analytical approach, while discerning the material's microstructure requires a different perspective.

4.6.3. Surface Related Properties

The surface of a material is susceptible to oxidation and corrosion. In materials produced by powder metallurgy, especially those with a high porosity rate, the formation of fluid within the pores and its subsequent accumulation can accelerate the corrosion process. Based on our observations, it can be inferred that materials sintered

under optimal conditions demonstrate the greatest resistance to environmental stressors [94].

PART 5

METHODOLOGY

5.1. MATERIALS

The investigation has developed innovative composite materials by incorporating stainless steel 316L with additions of titanium (Ti), and zirconium (Zr). All the samples were created using powder metallurgy techniques. The sizes and purity levels of the powders used are detailed in Table 5.1. Figure 5.1 depicts the step-by-step process employed in the fabrication of these samples.

Table 5.1. The sizes purities and density of the powders.

	Elemental powders	size (μm)	Purity %	Density (g/cm^3)	Supplied Company
1	SS316L	<149	99.9	7.95	Höganäs, USA
2	Ti	<45	96.5%	4.54	Aldrich, Germany
3	Zr	<80	99.5%	6.51	Nanograafi, Turkey

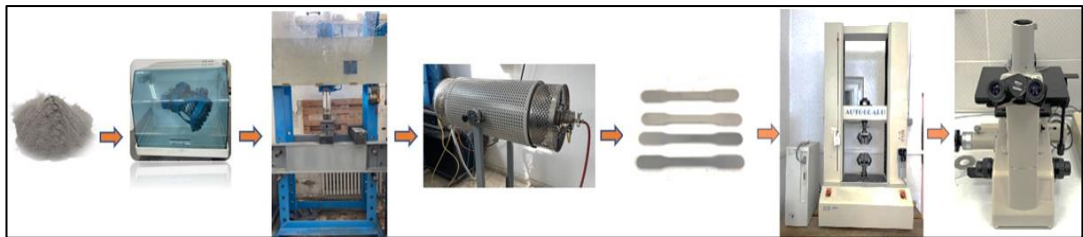


Figure 5.1. The sequence of operations of this study.

Table 5.2 Chemical compositions of powder metal steels.

Composition	
316L	1310°C – 2Hr
316L+0.2Ti	1310°C – 2Hr
316L+0.5Ti	1310°C – 2Hr
316L+1Ti	1310°C – 2Hr
316L+0.2Zr	1310°C – 2Hr
316L+0.2Ti+0.2Zr	1310°C – 2Hr

5.2. MIXING

Before initiating the mixing process, the powders were measured using a RADWAG AS-60-220 C/2 precision scale, which offers a measuring accuracy of 0.0001 g.



Figure 5.2. the RADWAG AS-60-220 C/2 weigh device.

Using a TURBULA T2F apparatus (Willy A. Bachofen AG, Muttenz, Switzerland), which operates on the principle of three-dimensional motion, each powder composition was carefully formulated and mixed for a duration of one hour.

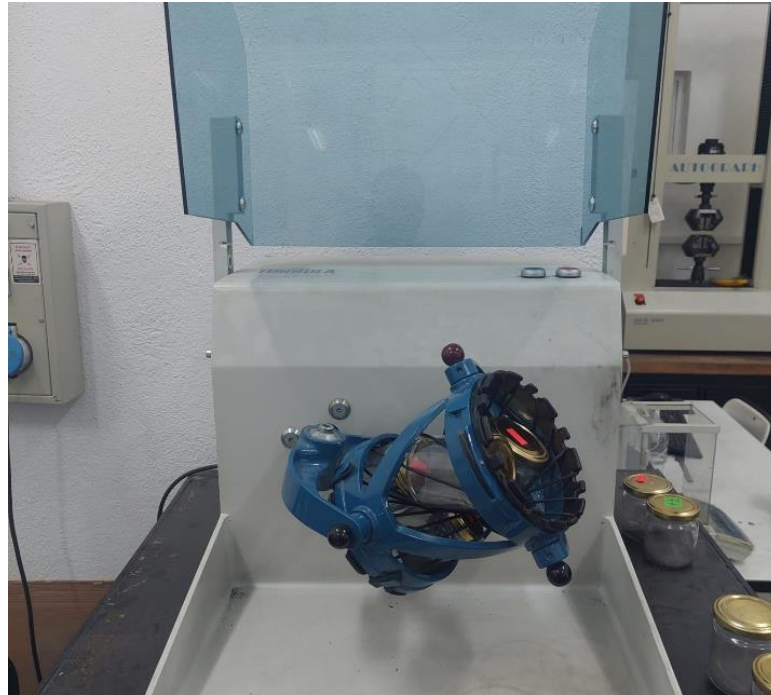


Figure 5.3. mixing TURBULA T2F device

5.3. PRESSING

The powders were meticulously compressed to achieve the desired shape for the tensile test specimen, as specified by the ASTM E8M standards[66]. This was achieved using a hydraulic press from Hidroliksan with an impressive capacity of 100 Tons. The pressing pressure was expertly set at an impressive 750 MPa.

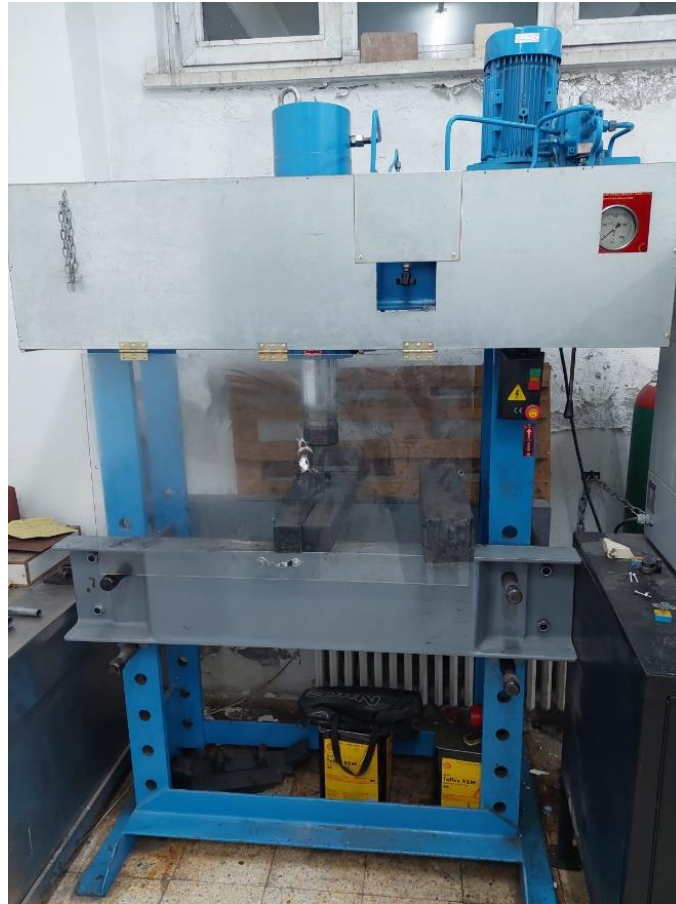


Figure 5.4. Hydraulic pressing (Hidroliksan machine).

5.4. SINTERING

After pressing, the material underwent sintering in an Argon atmosphere, heated at a rate of 5°C per minute until it reached a final temperature of 1310°C . In the second phase of the experiment, the samples were cooled down to room temperature from this peak temperature at a rate of 5°C per minute.



Figure 5.5. Sintering device.

Figure 5.6 shows the samples after sintering.



Figure 5.6 Produced samples after sintering.

5.5. DENSITY MEASUREMENT

The densities of the specimens were determined using the Radwag density kit, following the ASTM B 328-96 standard[67], which is based on the Archimedes principle.

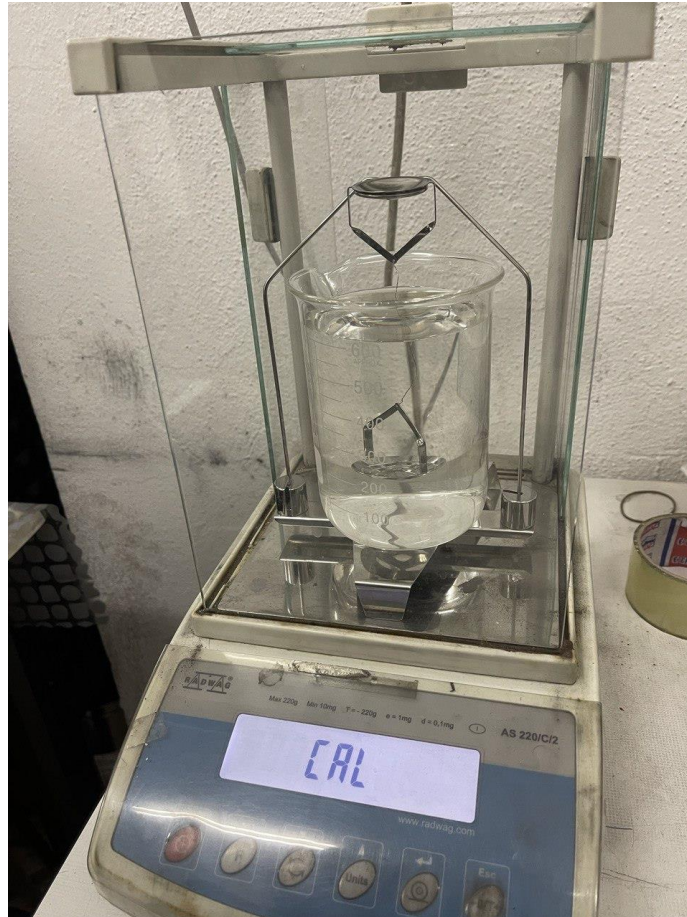


Figure 5.7. The Radwag density kit.

5.6. TENSILE TEST

The sintered samples underwent tensile testing using a SHIMADZU tensile testing machine with a 50 KN capacity (Shimadzu, Tokyo, Japan), operating at a crosshead speed of 1 mm/min.



Figure 5.8. SHIMADZU tensile test device.

Stress-strain graphs were obtained from each individual test. Through careful analysis of these graphs, we successfully quantified the yield strength (0.2%), tensile strength, and strain values of the samples. Furthermore, this analysis enabled us to determine the extent of variation in mechanical properties resulting from changes in the chemical composition.

5.7. HARDNESS TEST

The microhardness of these components was measured using a SHIMADZU hardness testing machine (MCT-W, Shimadzu, Tokyo, Japan), applying an HV0.5 load for a duration of 15 seconds. The hardness value for each sample was determined by calculating the average of five individual hardness tests.



Figure 5.9. SHIMADZU hardness test device.

5.8. OPTICAL MEASUREMENTS

The cutting samples were molded in cold molding using epoxy and silicone mold. Before using the optical microscope, the sample surfaces underwent a detailed preparation process. This included polishing with a range of abrasive papers of varying mesh sizes, from 400 to 7000 meshes, progressing from coarse to fine. Afterward, a $0.3 \mu\text{m}$ Al_2O_3 solution was employed for the final polishing. The samples were then etched for a duration of 3 seconds in a solution composed of 2% nitric acid and 98% ethyl alcohol. Finally, each sample was thoroughly cleaned with distilled water and ethyl alcohol, followed by a meticulous drying process using hot air.

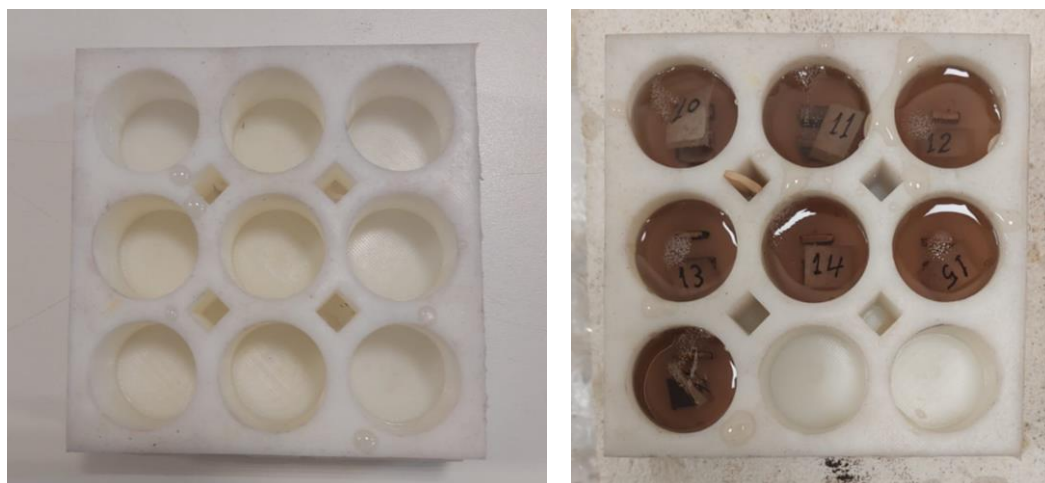


Figure 5.10. cold molding mold.



Figure 5.11. grinding and polishing device.

The optical microscopy examination was performed using the notably precise and high-quality Nikon ECLIPSE L150 microscope, manufactured in Melville, New York, USA. To determine the grain sizes of the composites, the mean linear intercept method was employed [68].

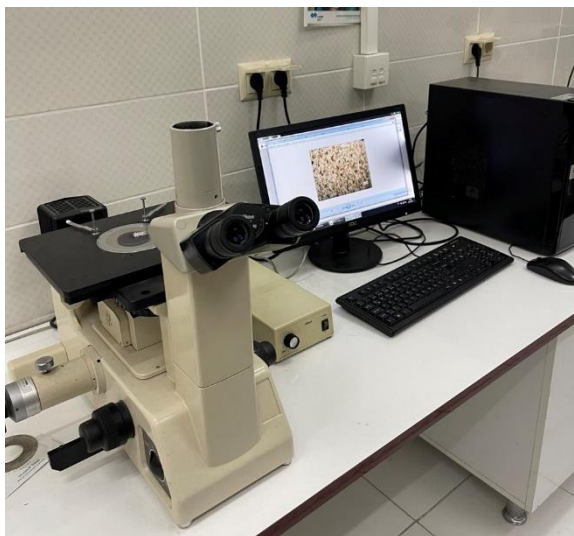


Figure 5.12. Nikon ECLIPSE L150 microscope.

5.9. CORROSION TEST

Before the corrosion test, the samples were cut to the required size and then copper wire was soldered to the samples in order to ensure conductivity of the samples with the corrosion unit, and then they were cold molded with epoxy resin to provide insulation.

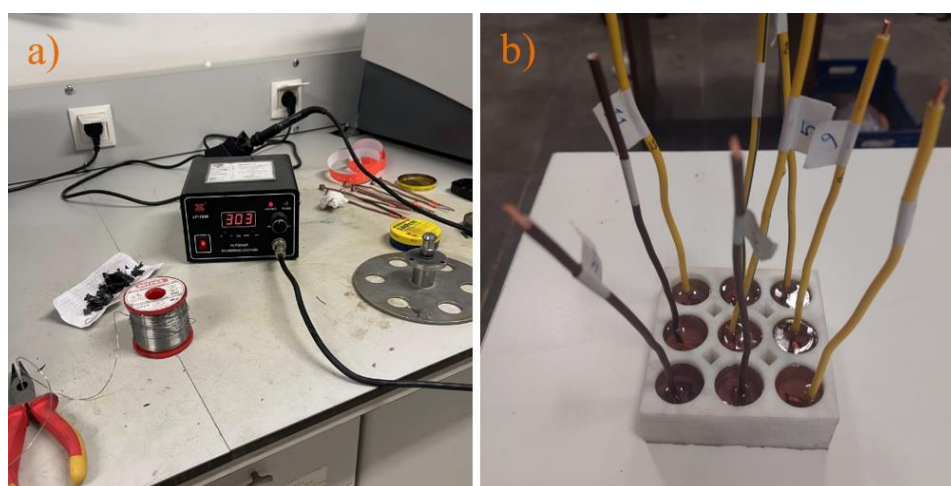


Figure 5.13. a) Soldering station device. b) Cold molding for corrosion samples.

A variety of abrasive paper meshes were used to prepare the samples (400, 600, 800, 1000, 1500, 2000 and 2500 meshes, coarse to fine). After the grinding the conductivity of samples were checked via voltmeter device.

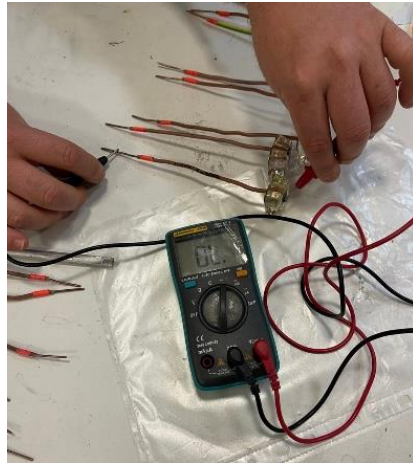


Figure 5.14. Checking the conductivity of corrosion samples.

The SBF were prepared as the chemical composition at pH 7.4 and T = 36.6 °C as shown in Table 5.3

Table 5.3. Chemical composition of simulated body fluid (SBF)[95].

Reagent	Amount
NaCl (g)	8.035
NaHCO ₃ (g)	0.355
KCl(g)	0.225
K ₂ HPO ₄ .3H ₂ O(g)	0.231
MgCl ₂ .6H ₂ O(g)	0.311
CaCl ₂ (g)	0.292
Na ₂ SO ₄ (g)	0.072
Tris (hydroxymethyl) aminomethane(g)	6.118
1M HCl (ml)	40



Figure 5.15. prepared the (SBF) solution.

After cleaning the test surface, the samples were washed with ethyl alcohol and distilled water. To prepare for corrosion testing, a large piece of adhesive tape with a 0.25 cm² diameter hole was applied to the specimen's surface. This step aimed to minimize potential negative effects from the epoxy bonding areas. The corrosion tests for all specimens were conducted in a controlled environment. The potentiodynamic polarization experiments were performed in a simulated body fluid (SBF) solution at a temperature of 37 °C, using a computer-operated Gamry model PC4/300 mA potentiostat/galvanostat for DC105 corrosion research. The electrochemical cell for these experiments was configured with three electrodes: a saturated calomel reference electrode (Ag/AgCl), a graphite counter electrode, and the working electrode. The capillary lugging was carefully positioned as close to the working electrode as possible to ensure minimal power loss in the setup.

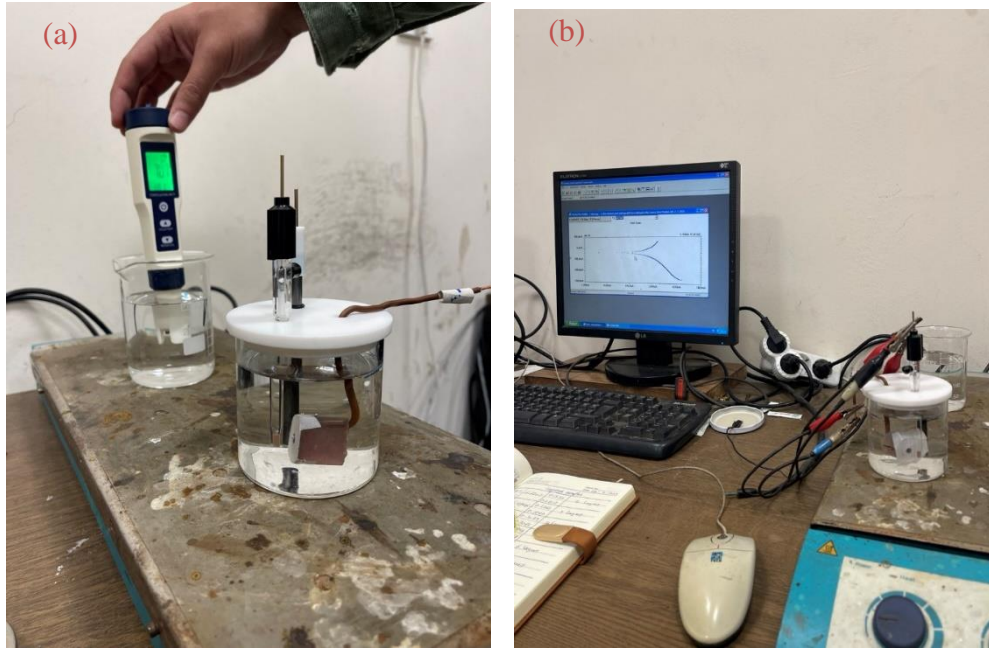


Figure 5.16. a) Three-electrode electrochemical cell, b)Tafel corrosion set.

5.10. WEAR TEST

A variety of abrasive paper meshes were used to prepare the samples for the wear test (400, 600, 800, 1000, 1500, 2000, and 2500 meshes, coarse to fine).

4D-ECN model tribometer device was used for wear tests. The wear test was carried out at 37 °C in SBF solution under 10N and 20N loads, with stroke of 10 mm, a total of 100 meters of sliding distance for each load, and 0.04 m/s sliding speed. Alumina balls with 6mm diameter were used for wear test.

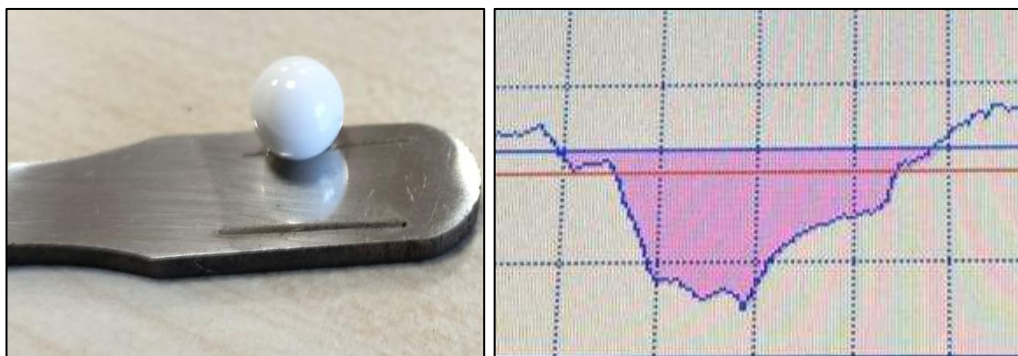


Figure 5.17. Wear test specimen, Al₂O₃ ball and wear area loss measurement.



Figure 5.18. Wear test device.

PART 6

RESULTS AND DISCUSSION

6.1. MICROSTRUCTURE

The microstructure images of the samples produced via the PM technique were taken at a pressure of 750 MPa and sintered in an atmosphere of argon at a temperature of 1310°C for two hours. Figure 6.1. to Figure 6.6. show the optical microscope images of the samples produced by the PM method before and after the alloying elements (Ti and Zr) were added.

It can be observed from the microscopic images that when 0.2 of Ti and Zr were added to stainless steel, the grain size in the microstructure became smaller, and when the amount of alloying elements (Ti and Zr) was increased, an increase in the grain size was observed.

Zhai et al [96] studied the grain refinement of 316L stainless steel through in-situ alloying with Ti in additive manufacturing. They reported that the Ti addition can significantly promote grain refinement (from 16.7 to 0.8 μm) without introducing undesirable intermetallic phases in selective laser-melted 316L. The Ti-rich solutes at the solid/liquid interface activated heterogeneous nucleation, thus achieving grain refinement.

Microstructure images of the samples produced with the PM technique were taken at a pressure of 750 MPa and sintered for two hours at 1310 C in an argon atmosphere. Figures 6.1-6.6 show optical microscope images of samples produced by the PM method before and after adding alloying elements (Ti and Zr). It can be seen from the microscopic images that when 0.2 Ti and 0.2Zr are added to 316L stainless steel, the grain size in the microstructure decreases, and when 1% Ti is added as an alloying

element, the grain size increases. Additionally, when Figures 3 and 4, which show the optical microscope images taken from all 316 L compositions produced, are examined, it is seen that structures consistent with similar findings in the literature are formed.

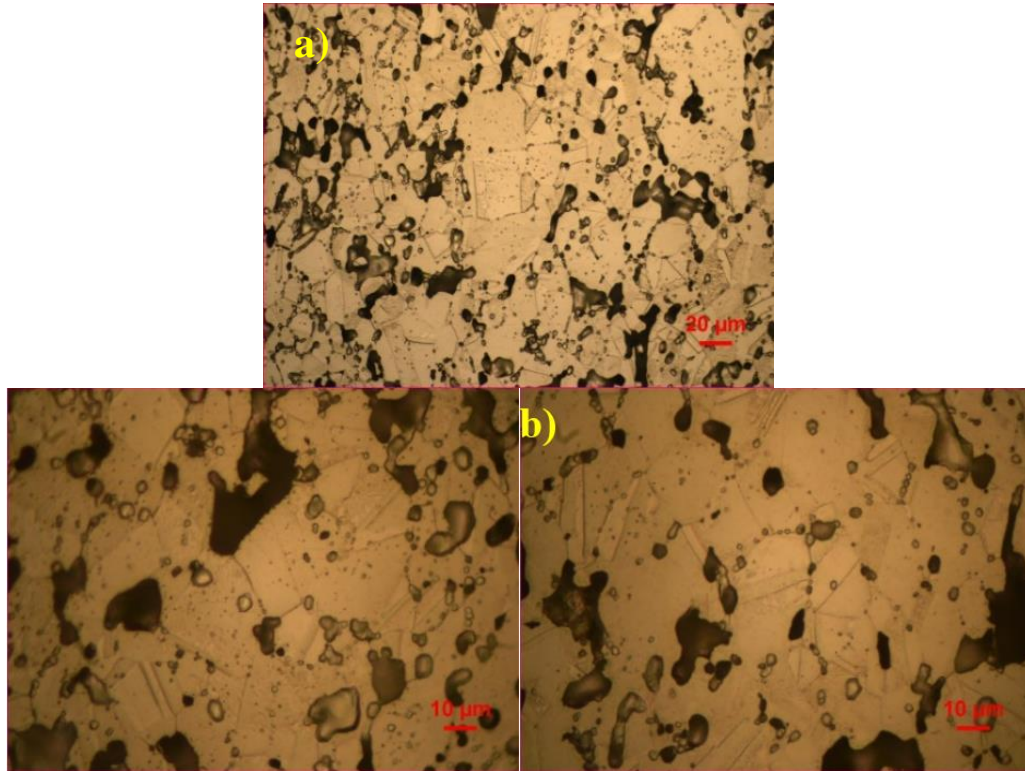


Figure 6.1. The optical micrographs of 316L (a) 500x. (b) 1000x.

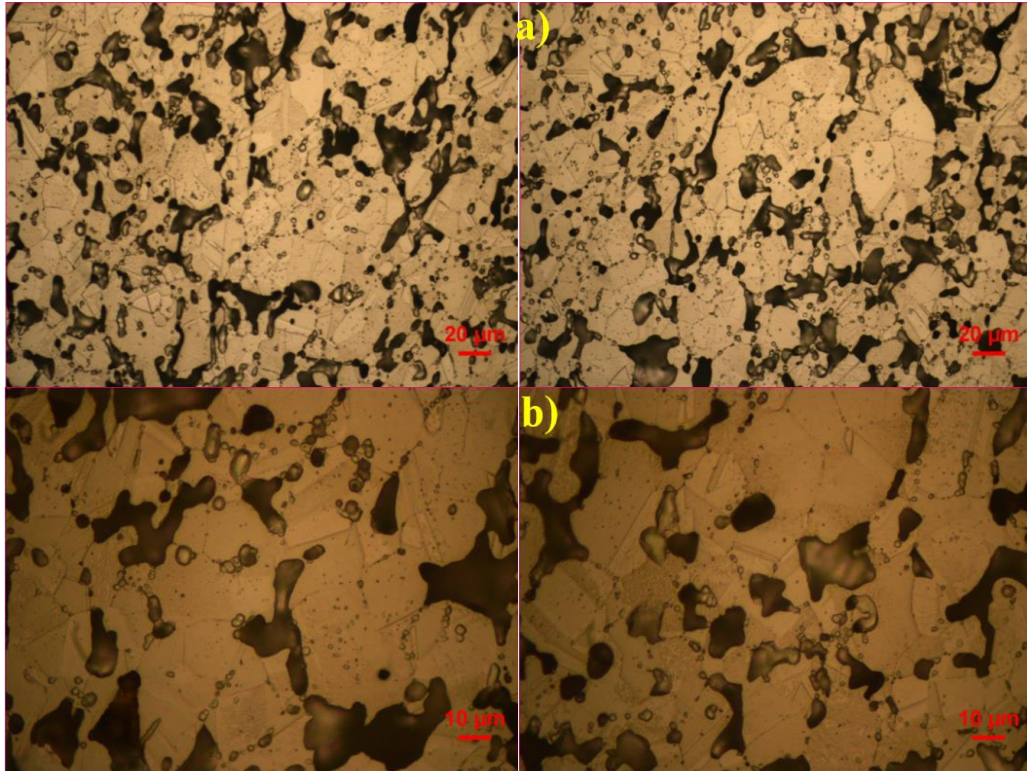


Figure 6.2. The optical micrographs of 316L+0.2Ti (a) 500x. (b) 1000x.

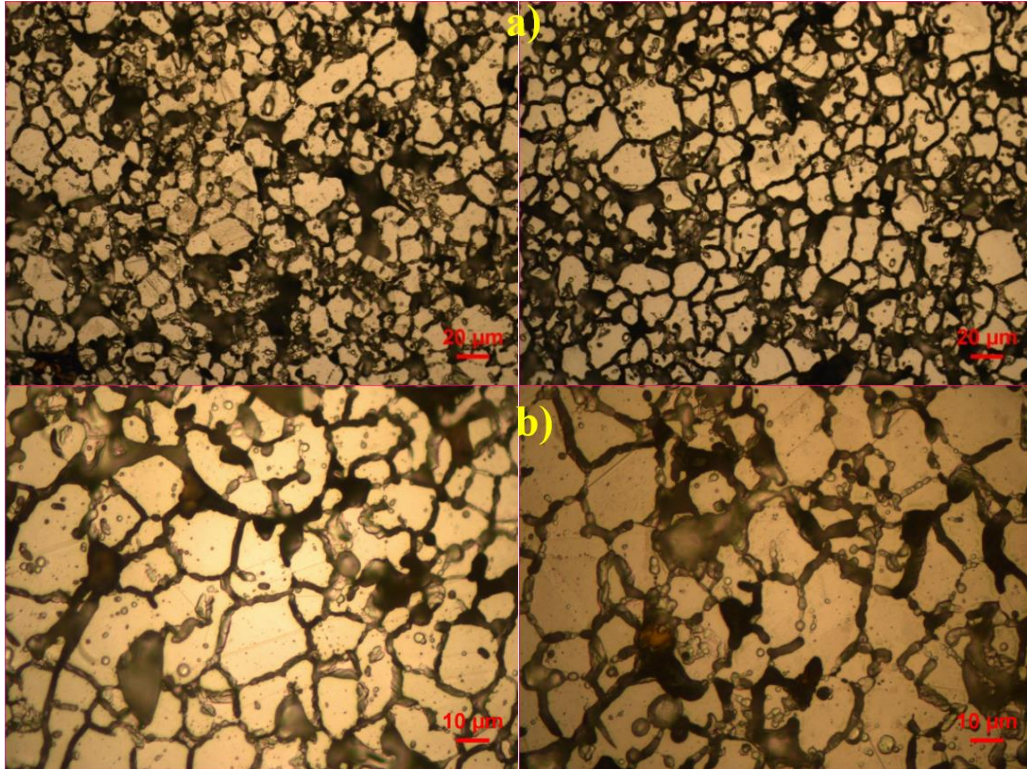


Figure 6.3. The optical micrographs of 316L+0.5Ti (a) 500x. (b) 1000x.

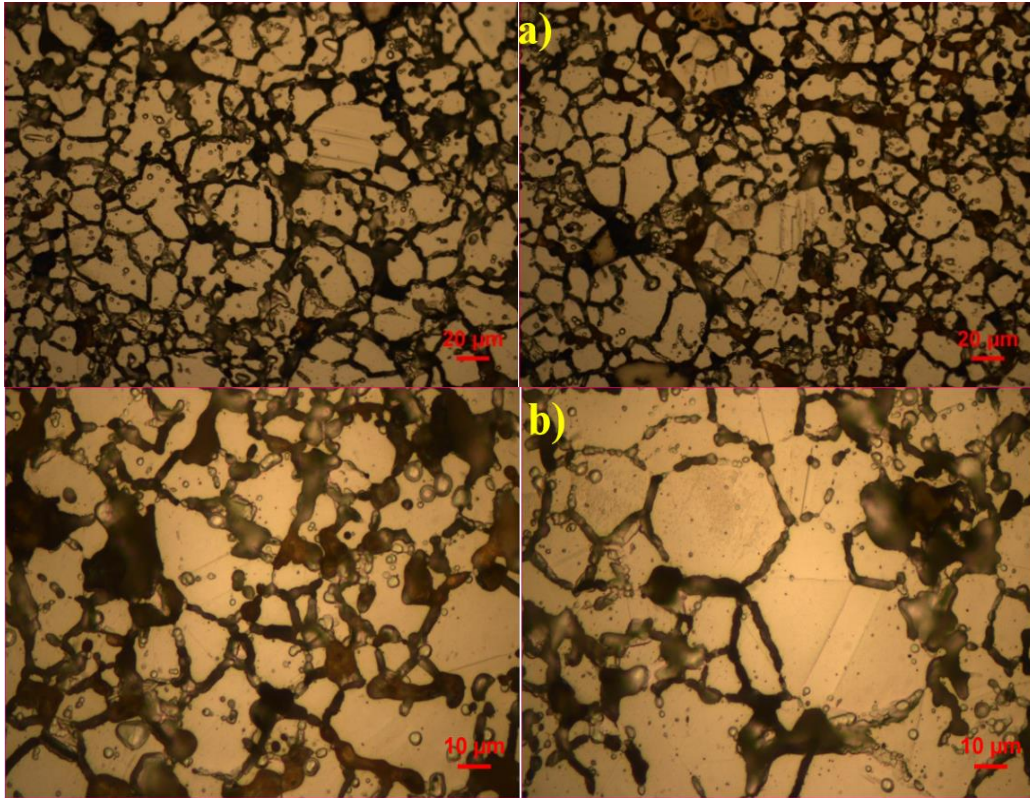


Figure 6.4. The optical micrographs of 316L+1Ti (a) 500x. (b) 1000x.

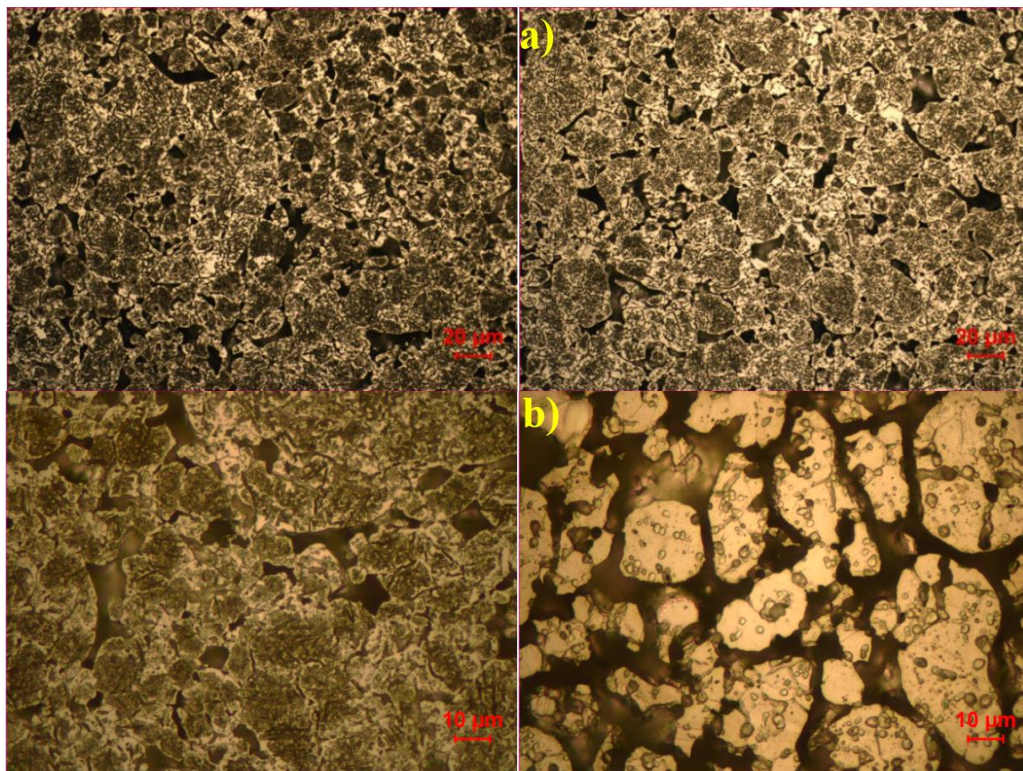


Figure 6.5. The optical micrographs of 316L+0.2Zr (a) 500x. (b) 1000x.

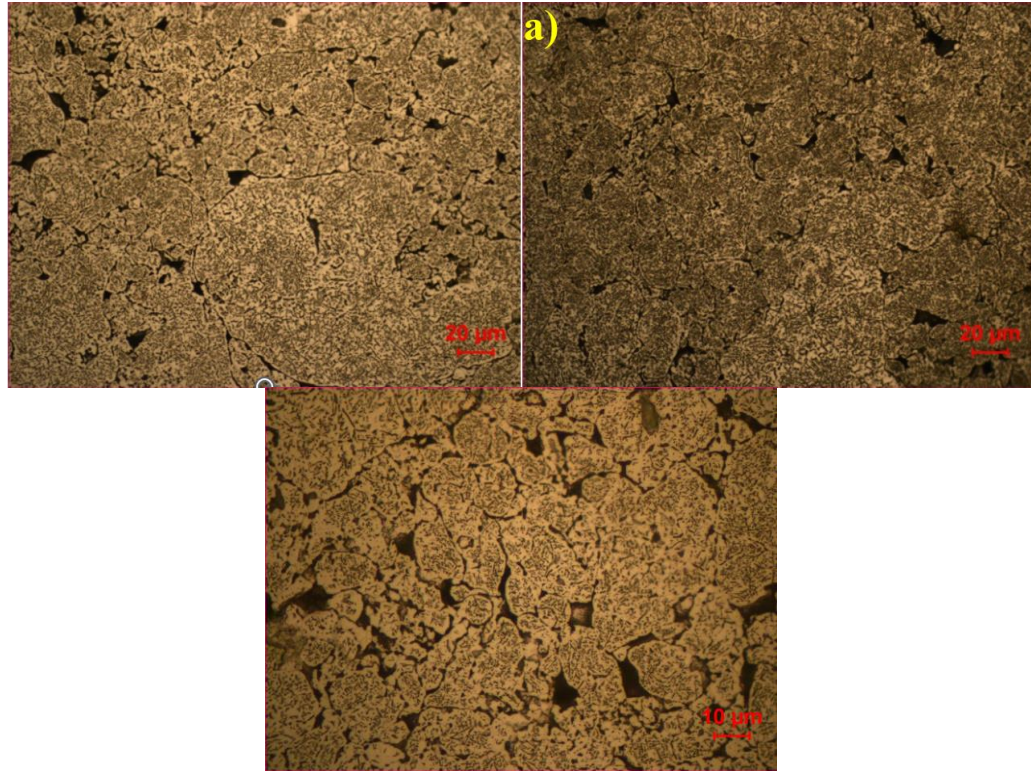


Figure 6.6. The optical micrographs of 316L+0.2Ti+0.2Zr (a) 500x. (b) 1000x.

6.2. MECHANICAL PROPERTIES

The mechanical properties of the produced alloys were determined by tensile and hardness measurements. Tensile test and density measurement results are given in Table 6.1, which is based on the data obtained.

Looking at the tensile results given in Table 6.1, the maximum tensile strength of unalloyed powder metal 316L stainless steel was measured as 263 MPa. When Ti element was added to unalloyed powder metal 316L stainless steel at the rates of 0.2%, 0.5% and 1.0% by weight, respectively, the value of the maximum tensile strength decreased. The maximum tensile strength was 320 MPa when 0.2% Ti was added, 290 MPa when 0.5% Ti was added, and 247 MPa when 1% Ti was added. In the study, 115 MPa tensile strength was obtained in the 316L+0.2% Zr alloy created to measure the effect of Zr addition alone. The 316L+0.2Ti+0.2 Zr alloy, which was created to see the synergistic effect of Ti and Zr elements, showed a very good result and showed a tensile strength of 415 MPa. Considering the density values obtained, a porosity of 9.19 was obtained in the 316L sample. The porosity value was found to be a very low

value of 15% in the sample containing 1% Ti. A very low porosity of 8.27 was measured in the 316L+0.2Ti+0.2 Zr alloy, which is directly proportional to the tensile strength.

When the percentage of Ti and Zr was enriched (0.2-0.2% by weight), the tensile strength of the alloy increased, and the highest value was 166 MPa. That is, the tensile strength of the Alloy increased by 63.06% compared to Alloy I, where no alloying elements were added. The elongation percentage in Alloy 2 is at the highest level compared to the others, at 27%. However, when the Ti alloying element addition was increased to 1 percent by weight, a decrease in tensile strength and hardness values was observed.

Türkmen et al. [97] in their study examining the effect of Mn and Ti elements added to 316L stainless powder metal steel, observed an increase in porosity values and a decrease in tensile values when Ti addition exceeded 1.5% level.

This decrease in tensile strength and hardness values can be attributed to the increase in the size of the precipitates formed at the matrix and grain boundaries, the increase in the number of pores and the increase in the grain size of the material due to the large size of the precipitates. It does not inhibit dislocation movement sufficiently compared to small precipitates. Grain boundaries, like precipitates, also inhibit dislocation movement. Similarly, coarse-grained materials have shorter grain boundaries. Decreasing grain boundary length resulted in decreased strength due to the reduction of barriers preventing dislocation movement. Another reason for the decrease in strength can be expressed as an increase.

Zhai et al. [96] studied the Grain refinement of 316L stainless steel through in-situ alloying with Ti in additive manufacturing. They reported that the With the addition of Ti, the ultimate tensile strength (UTS) was enhanced from 704 MPa for 316L to 817 MPa for 316L-1.5Ti. In addition, the microhardness of 316L increases with the addition of Ti. With a 0.3 wt% Ti addition, the microhardness was slightly increased to 242.6 ± 7.5 HV. With 1 and 1.5 wt% Ti additions, the microhardness was further

increased to 264.4 ± 9.0 and 275.9 ± 25.0 HV, respectively. The microhardness of SLM 316L-3Ti increased significantly, measured at 523.2 ± 42.4 HV.

When Figure 6.7 is examined, the hardness value of 316L stainless steel was 99 Hv0.5, but with the addition of 1% Ti, this value decreased to 93 Hv0.5. In the 316L0.2Ti+0.2Zr alloy created for synergistic interaction, this value increased to 163 Hv0.5. It is thought that the grain size and the precipitates formed are effective in this formation.

Pandya et al. [98] investigated the effect of sintering temperature on the densification response and mechanical behavior of 316 L stainless steel. They reported that the hardness changed from 97 HV to 126 HV as the density increased from 83% to 90%. In another study, the measured hardness of PM 316 L stainless steel samples with 15.6% porosity was 160 HV; this was higher than the alloys studied [99].

Table 6.1. Mechanical properties of PM steel samples.

compositions	UTS (MPa)	Elongation (%)	Theoretical Density (g/cm³)	Experimental Density (g/cm³)	Porosity (%)
316L	263	25	7.85	7.1282	9.19
316L+0.2Ti	320	27	7.8453	7.0861	9.67
316L+0.5Ti	290	21	7.8384	6.6788	14.79
316L+1Ti	247	17	7.8269	6.6525	15.00
316L+0.2Zr	115	3	7.8473	6.9748	11.11
316L+0.2Ti+0.2Zr	415	7	7.8427	7.1937	8.27

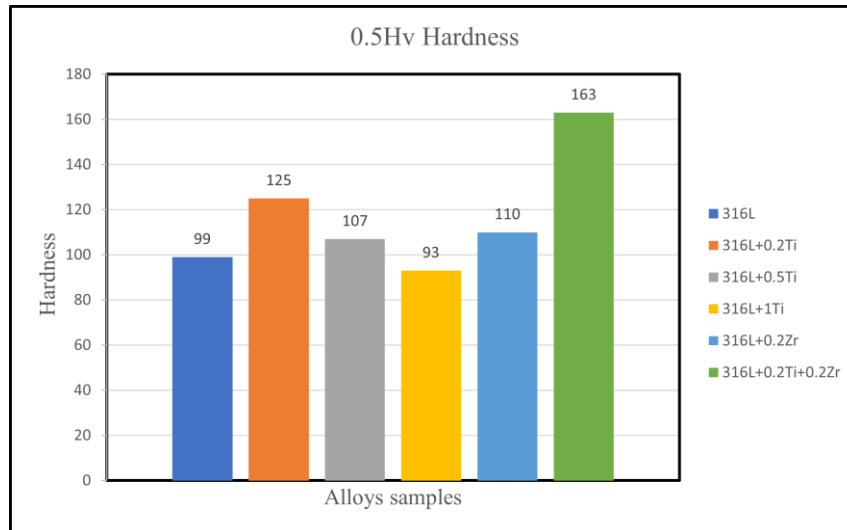


Figure 6.7 Microhardness of pm samples.

6.3. CORROSION TEST RESULTS

In Hang (human body) solutions at 37°C, Pavapootanont et al [100]. examined the corrosion characteristics of 316L stainless steels. Although the passive current density of these three kinds of steels declined as the Titanium content increased, both the pitting potentials and primary passive potentials improved. Titanium improved the steel's overall corrosion and pitting corrosion resistance in all three solutions. In another study, 316L stainless steels in the Hang solution was studied by Wang et al. to determine the ideal Zr concentration for the steel's microstructure, phase, and electrochemical behaviors.

A finer grain size were present in the sample with 0,2 % Ti- 0,2 % Zr. The Ti addition also improved the low alloy steel's charge transfer resistance, suggesting the sample had outstanding electrochemical reaction inhibition and corrosion resistance.

When Figure 6.8 and Table 6.2 are examined, the alloy containing 316L+0.2Ti+0.2Zr showed the best corrosion resistance. It is an expected result that corrosion resistance increases with a certain amount of Ti and Zr content [101] . Studies in the literature also support these results. Polarization and surface resistances were significantly higher for the alloy with low Ti ($\geq 0.5\%$) concentration. The potentiostatic polarization curves of the corroded samples showed that the current densities of the samples

initially decreased and then stabilized at low positive current density due to passive film formation. The current densities of the samples containing Ti and Zr were significantly lower than the current density of the 316L sample and did not show larger fluctuations.

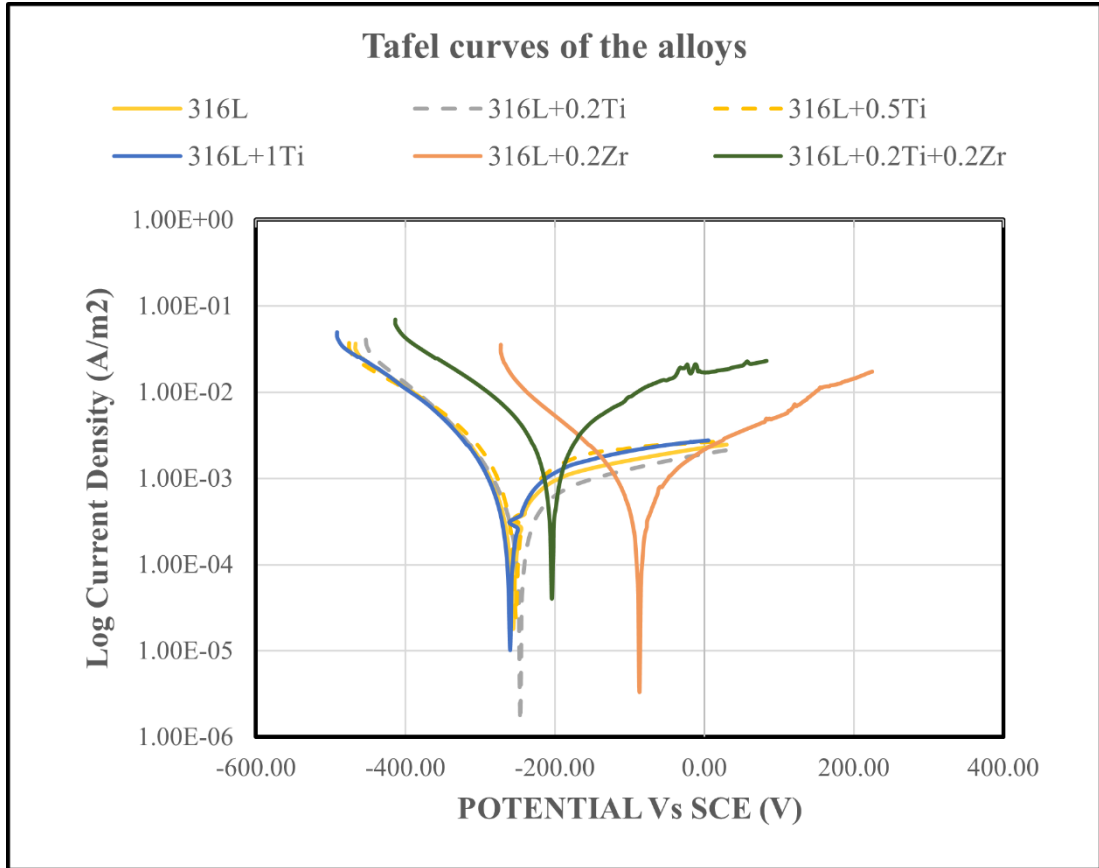


Figure 6.8. Tafel curves of the alloys.

Table 6.2. E_{corr}, I_{corr}, and corrosion rate values of PM steel samples.

Composition	E _{corr} (mV)	I _{corr} (μA/cm ²)	CR (mm/year)
316L	-98.7	13.90e-6	0.3911
316L+0.2Ti	-246	870e-9	0.1977
316L+0.5Ti	-253	2.4e-6	0.5791
316L+1Ti	-260	1.190e-6	0.2880
316L+0.2Zr	-87.10	2.33e-6	0.5382
316L+0,2Ti+0,2Zr	-94.2	805e-9	0.1900

6.4. WEAR TEST RESULTS

316L matrix samples, which are also used as biomaterials in the study, were subjected to abrasion testing in body fluid. The wear test was carried out under 10 and 20 N loads, at a wear distance of 100 meters and at a sliding speed of 0.04m/sec. Al_2O_3 ball with a diameter of 6 mm, which is also used as a biomaterial, was used as abrasive. The data obtained in the wear test gave parallel results with the tensile and hardness results. Figure 6.9 shows the wear test results under 20N load. After the wear test, the total volume loss was measured by multiplying the area loss measured with the surface profilometer device by the trace length of 10 mm. When the measurements were examined, the highest volume loss at 20N load was in the sample containing 1%Ti. The 316L+0.2Ti+0.2Zr sample, which had the highest hardness and tensile results, had the lowest volume loss with 0.09 mm^3 .

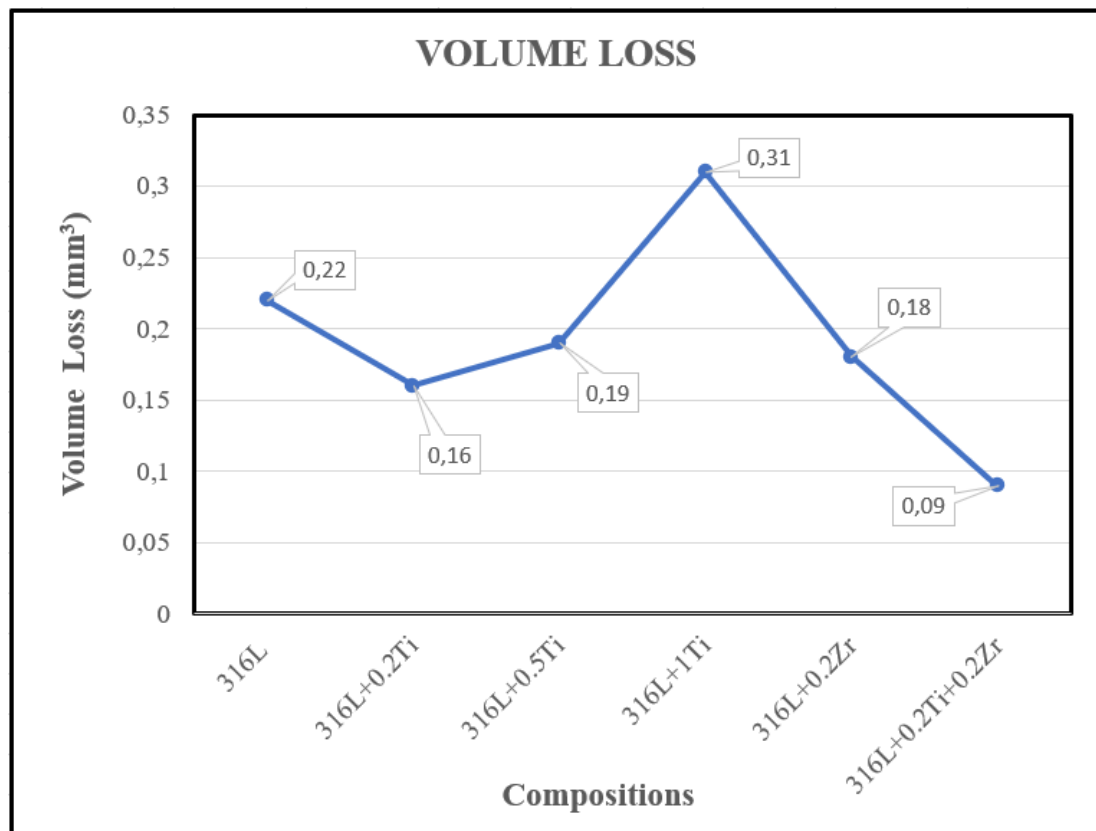


Figure 6.9. Wear volume loss data of samples examined under 20N load.

PART 7

CONCLUSION

In this study, the effect of adding Ti and Zr elements to 316L stainless steel alloy produced by powder metallurgy method was investigated for two hours under cold pressure (750 MPa) and sintering temperature (1310 °C) in argon atmosphere and the following results were obtained:

- It can be seen from the microscopic images that when 0.2 Ti and 0.2Zr are added to 316L stainless steel, the grain size in the microstructure decreases, and when 1% Ti is added as an alloying element, the grain size increases.
- When Ti and Zr (0.2 wt%) by weight are added to the original steel alloy without additives, the tensile strength, yield strength and hardness of the steel alloy increase due to the precipitation of the elements, and these precipitates are thought to inhibit grain growth.
- When Ti and Zr are added together at the same weight percentage (0.2 wt%), better properties are obtained than adding Ti or Zr via monotherapy, because all kinds of precipitates are formed when the two elements TiC(N) are added together. It can be predicted that ZrC(N) and TiZrC(N) are formed during recrystallization and sintering, which prevent the expansion of boundaries.
- When Ti and Zr (0.2% by weight) are added to the original steel alloy without additives, the tensile strength, yield strength and hardness of the steel alloy increase due to the precipitation of the elements, and these precipitates inhibit grain growth.

- Figure 6.8 and Table 6.2 are examined, the alloy containing 316L+0.2Ti+0.2Zr showed the best corrosion resistance. It is an expected result that corrosion resistance increases with a certain amount of Ti and Zr content.
- When the wear measurements were examined, the highest volume loss at 20N load was in the sample containing 1%Ti. The 316L+0.2Ti+0.2Zr sample, which had the highest hardness and tensile results, had the lowest volume loss with 0.09 mm³.

REFERENCES

1. Khoshnaw, F., Yamanoglu, R., Basci, U. G., and Muratal, O., "Pressure assisted bonding process of stainless steel on titanium alloy using powder metallurgy", *Materials Chemistry And Physics*, 259: 124015 (2021).
2. Lee, J. G. and Lee, M. K., "Microstructure and mechanical behavior of a titanium-to-stainless steel dissimilar joint brazed with Ag-Cu alloy filler and an Ag interlayer", *Materials Characterization*, 129 (February): 98–103 (2017).
3. Gunduz, S., Erden, M. A., Karabulut, H., and Turkmen, M., "The Effect of Vanadium and Titanium on Mechanical Properties of Microalloyed PM Steel", *Powder Metallurgy And Metal Ceramics*, 55 (5–6): 277–287 (2016).
4. Kipouros, G. J., Caley, W. F., and Bishop, D. P., "On the advantages of using powder metallurgy in new light metal alloy design", *Metallurgical And Materials Transactions A: Physical Metallurgy And Materials Science*, 37 (12): 3429–3436 (2006).
5. Chen, J., Lv, M. yang, Tang, S., Liu, Z. yu, and Wang, G. dong, "Influence of cooling paths on microstructural characteristics and precipitation behaviors in a low carbon V-Ti microalloyed steel", *Materials Science And Engineering A*, 594: 389–393 (2014).
6. Baker, T. N., "Processes, microstructure and properties of vanadium microalloyed steels", *Materials Science And Technology*, 25 (9): 1083–1107 (2009).
7. Xiao, D. H., Yuan, T. C., Ou, X. Q., and He, Y. H., "Microstructure and mechanical properties of powder metallurgy Ti-Al-Mo-V-Ag alloy", *Transactions Of Nonferrous Metals Society Of China (English Edition)*, 21 (6): 1269–1276 (2011).
8. Anand, S., Schade, R. R., Bendetti, C., Kelly, R., Rabin, B. S., Krause, J., Starzl, T. E., Iwatsuki, S., and Van Thiel, D. H., "Idiopathic Hemochromatosis and Alpha-1-Antitrypsin Deficiency: Coexistence in a Family with Progressive Liver Disease in the Proband", *Hepatology*, 3 (5): 714–718 (1983).
9. Erden, M. A., Erer, A. M., Odabaşı, Ç., and Gündüz, S., "The Investigation of the Effect of Cu Addition on the Nb-V Microalloyed Steel Produced by Powder Metallurgy", *Science Of Sintering*, 54 (2): 153–167 (2022).
10. Gündüz, S., Erden, M. A., Karabulut, H., and Türkmen, M., "Effect of the addition of niobium and aluminium on the microstructures and mechanical properties of micro-alloyed pm steels", *Materiali In Tehnologije*, 50 (5): 641–648 (2016).

11. Huang, H. Y., "Ce d M us pt", *Nanotechnology*, 0–22 (2017).
12. "AN INVESTIGATION OF THE EFFECT OF MN AND ZR ADDITION ON THE MICROSTRUCTURE , MECHANICAL AND CORROSION PROPERTIES OF TI6AL4V DEPARTMENT OF MECHANICAL Mohamed Erhaima Emahmed ERHAIMA Thesis Advisor Assist . Prof . Dr . Harun ÇUĞ", (2020).
13. Coovattanachai, O., Lasutta, P., Tosangthum, N., and Krataitong, R., "Analysis of Compaction and Sintering of Stainless Steel Powders", 33 (2): 293–300 (2006).
14. H. M. Cobb, *The history of stainless steel*. ASM International, 2010.
15. J. R. Davis, *Stainless steels*. ASM international, 1994.
16. J. R. Davis, *Alloy digest sourcebook: stainless steels*. ASM international, 2000.
17. Godbole, N., Yadav, S., Ramachandran, M., and Belemkar, S., "A review on surface treatment of stainless steel orthopedic implants", *International Journal Of Pharmaceutical Sciences Review And Research*, 36 (1): 190–194 (2016).
18. T. K. Painkra, K. S. Naik, R. K. Nishad, P. K. Sen, "Review about high performance of Austenitic Stainless Steel", *International Journal For Innovative Research In Science & Technology*, 1 (6): 93–99 (2014).
19. Andersen, P. J., "1.3.3B – Stainless Steels", *Biomaterials Science: An Introduction to Materials in Medicine*, Fourth Edi. Ed., *Elsevier*, 249–255 .
20. Zivic, F., Affatato, S., Trajanovic, M., Schnabelrauch, M., Grujovic, N., and Choy, K. L., .
21. Dutta, S. K., "Different Types and New Applications of Stainless Steel", *Stainless Steel*, 62 (10): 5 (2018).
22. Randelović, S., "Manufacturability of biomaterials", *Biomaterials In Clinical Practice: Advances In Clinical Research And Medical Devices*, 633–658 (2017).
23. Randjelović, S., Manić, M., Trajanović, M., Milutinović, M., and Movrin, D., "The impact of die angle on tool loading in the process of cold extruding steel", *Materiali In Tehnologije*, 46 (2): 149–154 (2012).
24. Suprihanto, A., "Magnetic Properties of Austenitic Stainless Steel 316l and 316lvm after High Temperature Gas Nitriding Treatment", *Rotasi*, 19 (2): 72 (2017).
25. Borgioli, F., "From austenitic stainless steel to expanded austenite-s phase: Formation, characteristics and properties of an elusive metastable phase", *Metals*, 10 (2): (2020).

26. Tadepalli, L. D., Gosala, A. M., Kondamuru, L., Bairi, S. C., Subbiah, R., and Singh, S. K., "A review on effects of nitriding of AISI409 ferritic stainless steel", *Materials Today: Proceedings*, 26 (xxxx): 1014–1020 (2019).
27. Cunat, P., "Alloying elements in stainless steel and other chromium-containing alloys", *International Chromium Development Association, ...*, 1–24 (2004).
28. Nilsson, J. O., "Super duplex stainless steels", *Materials Science And Technology (United Kingdom)*, 8 (8): 685–700 (1992).
29. Knyazeva, M. and Pohl, M., "Duplex Steels: Part I: Genesis, Formation, Structure", *Metallography, Microstructure, And Analysis*, 2 (2): 113–121 (2013).
30. Mesa, D. H., Toro, A., Sinatora, A., and Tschiptschin, A. P., "The effect of testing temperature on corrosion - erosion resistance of martensitic stainless steels", *Wear*, 255 (1–6): 139–145 (2003).
31. Park, J. Y. and Park, Y. S., "The effects of heat-treatment parameters on corrosion resistance and phase transformations of 14Cr-3Mo martensitic stainless steel", *Materials Science And Engineering: A*, 448–451: 1131–1134 (2007).
32. Singh, S. and Nanda, T., "Effect of Alloying and Heat Treatment on the Properties of Super Martensitic Stainless Steels", *Ijetsr.Org*, 1 (1): 6–9 (2013).
33. Zheng, H., Ye, X. N., Li, J. D., Jiang, L. Z., Liu, Z. Y., Wang, G. D., and Wang, B. S., "Effect of carbon content on microstructure and mechanical properties of hot-rolled low carbon 12Cr-Ni stainless steel", *Materials Science And Engineering: A*, 527 (27–28): 7407–7412 (2010).
34. Adamovic, D., Ristic, B., and Zivic, F., "Review of Existing Biomaterials-Method of Material Selection for Specific Applications in Orthopedics", *Biomaterials in Clinical Practice: Advances in Clinical Research and Medical Devices*, 47–99 (2017).
35. Kazior, J., Szewczyk-Nykiel, A., Pieczonka, T., Hebda, M., and Nykiel, M., "Properties of precipitation hardening 17-4 PH stainless steel manufactured by powder metallurgy technology", *Advanced Materials Research*, 811 (September): 87–92 (2013).
36. A. Ossowska, J. Ryl, and T. Sternicki, "Production and Properties of the Porous Layer Obtained by the Electrochemical Method on the Surface of Austenitic Steel," *Materials*, vol. 15, no. 3, p. 949, 2022.
37. Kocijan, A., Conradi, M., and Schön, P. M., "Austenitic and duplex stainless steels in simulated physiological solution characterized by electrochemical and X-ray photoelectron spectroscopy studies", *Journal Of Biomedical Materials Research - Part B Applied Biomaterials*, 100 B (3): 799–807 (2012).
38. Köse, C., Kaçar, R., Zorba, A. P., Bağırova, M., Abamor, E. Ş., and

- Allahverdiyev, A. M., "Interactions between fibroblast cells and laser beam welded AISI 2205 duplex stainless steel", *Medziagotyra*, 24 (2): 159–165 (2018).
39. Yang, K. and Ren, Y., "Nickel-free austenitic stainless steels for medical applications", *Science And Technology Of Advanced Materials*, 11 (1): 014105 (2010).
 40. Y.-O. Son, "Molecular mechanisms of nickel-induced carcinogenesis," *Endocrine, Metabolic & Immune Disorders-Drug Targets (Formerly Current Drug Targets-Immune, Endocrine & Metabolic Disorders)*, vol. 20, no. 7, pp. 1015–1023, 2020.
 41. Taxell, P. and Huuskonen, P., "Toxicity assessment and health hazard classification of stainless steels", *Regulatory Toxicology And Pharmacology*, 133 (June): 105227 (2022).
 42. Sudhakar, K. V. and Wang, J., "Fatigue behavior of vitallium-2000 plus alloy for orthopedic applications", *Journal Of Materials Engineering And Performance*, 20 (6): 1023–1027 (2011).
 43. Ha, H. Y., Lee, T. H., Bae, J. H., and Chun, D. W., "Molybdenum effects on pitting corrosion resistance of FeCrMnMoNC austenitic stainless steels", *Metals*, 8 (8): 1–13 (2018).
 44. Steels, C. U., "Metals The Effect of Electroslag Remelting on the Microstructure and Mechanical Properties of", 1–9 (2020).
 45. D. G. Poitout, "Biomaterials used in orthopedics," *Biomechanics and Biomaterials in Orthopedics*, Second Edition. pp. 13–19, 2016, doi: 10.1007/978-1-84882-664-9_2
 46. Qadri, S. A. R., Sasidhar, K. N., and Meka, S. R., "High nitrogen alloying of AISI 316 L stainless steel powder by nitriding", *Powder Technology*, 390: 456–463 (2021).
 47. Gündüz, S. and Çapar, A., "Influence of forging and cooling rate on microstructure and properties of medium carbon microalloy forging steel", *Journal Of Materials Science*, 41 (2): 561–564 (2006).
 48. Hashemi, P. M., Borhani, E., and Nourbakhsh, M. S., "A review on nanostructured stainless steel implants for biomedical application", *Nanomed. J*, 3 (4): 202–216 (2016).
 49. Gu, C., Liu, R., Wang, C., Sun, Y., and Zhang, S., "Effect of aluminum on microstructure and high-temperature oxidation resistance of austenitic heat-resistant steel", *Metals*, 10 (2): 1–8 (2020).
 50. Cadosch, D., "Biocorrosion and Aseptic Loosening of Metal Implants : Novel Pathophysiological Mechanisms", (2011).
 51. Manivasagam, G., Dhinasekaran, D., and Rajamanickam, A., "Biomedical

- Implants: Corrosion and its Prevention - A Review~!2009-12-22~!2010-01-20~!2010-05-25~!", *Recent Patents On Corrosion Science*, 2 (1): 40–54 (2010).
52. Gündüz, S., Karabulut, H., Erden, M. A., and Türkmen, M., "Microstructural effects on fatigue behaviour of a forged medium carbon microalloyed steel", *Materialpruefung/Materials Testing*, 55 (11–12): 865–870 (2013).
 53. Rahman, A., Thesis, V., Assoc, A., Mehmet, A., Erden, A., and Akgün, M., "Investigation of the Effect of Cr Addition on the Mechanical and Machinability Properties of Cr-Mo Steels Produced By Powder Metallurgy 2022 Master Thesis Biomedical Engineering", (2022).
 54. R. Narayan, *Encyclopedia of biomedical engineering*. Elsevier, 2018.
 55. Zhang, X. G., "Galvanic Corrosion", *Uhlig's Corrosion Handbook: Third Edition*, 123–143 (2011).
 56. Simsir, H., Akgul, Y., and Erden, M. A., "Hydrothermal carbon effect on iron matrix composites produced by powder metallurgy", *Materials Chemistry And Physics*, 242: 122557 (2020).
 57. Jalota, S., Bhaduri, S. B., and Tas, A. C., "Using a synthetic body fluid (SBF) solution of 27 mM HCO₃⁻ to make bone substitutes more osteointegrative", *Materials Science And Engineering C*, 28 (1): 129–140 (2008).
 58. Johnson, R. and Von Der Ohe, C. B., "Tribocorrosion of Passive Metals and Coatings", *Tribocorrosion Of Passive Metals And Coatings*, 441–474 (2011).
 59. Güner, A. T. and Meran, C., "Biomaterials Used in Orthopedic Implants", *Pamukkale University Journal Of Engineering Sciences*, 26 (1): 54–67 (2020).
 60. Shaw, B. A., "Corrosion within the human body: Prospects and problems with bioimplants", *Electrochemical Society Interface*, 17 (2): 29 (2008).
 61. Cai, B., Liu, Y., Tian, X., Wang, F., Li, H., and Ji, R., "An experimental study of crevice corrosion behaviour of 316L stainless steel in artificial seawater", *Corrosion Science*, 52 (10): 3235–3242 (2010).
 62. Akpanyung, K. V. and Loto, R. T., "Pitting corrosion evaluation: A review", *Journal Of Physics: Conference Series*, 1378 (2): (2019).
 63. Voisin, T., Shi, R., Zhu, Y., Qi, Z., Wu, M., Sen-Britain, S., Zhang, Y., Qiu, S. R., Wang, Y. M., Thomas, S., and Wood, B. C., "Pitting Corrosion in 316L Stainless Steel Fabricated by Laser Powder Bed Fusion Additive Manufacturing: A Review and Perspective", *Jom*, 74 (4): 1668–1689 (2022).
 64. Kamachi Mudali, U., Sridhar, T. M., and Baldev, R. A. J., "Corrosion of bio implants", *Sadhana - Academy Proceedings In Engineering Sciences*, 28 (3–4): 601–637 (2003).

65. Panda, A., Dobránsky, J., Jančík, M., Pandová, I., and Kačalová, M., "Advantages and effectiveness of the powder metallurgy in manufacturing technologies", *Metallurgija*, 57 (4): 353–356 (2018).
66. Kruzhanov, V. and Arnhold, V., "Energy consumption in powder metallurgical manufacturing", *Powder Metallurgy*, 55 (1): 14–21 (2012).
67. James, P. J., "Particle deformation during cold isostatic pressing of metal powders", *Powder Metallurgy*, 20 (4): 199–204 (1977).
68. Guven, Ş. Y., "Toz Metalurjisi ve Metalik Köpükler", *SDÜ Teknik Bilimler Dergisi*, 1 (2): 22–28 (2011).
69. Dogan, C., "METAL-POWDER PRODUCTION BY CENTRIFUGAL ATOMIZATION", *International Journal Of Powder Metallurgy*, 30 (4): pp.419-427 (1994).
70. A. Rawle, "Basic of principles of particle-size analysis," *Coatings Journal*, 86 (2): 58_65 (2003).
71. R. M. German and S. J. Park, "Handbook of Mathematical Relations in Particulate Materials Processing: Ceramics, Powder Metals, Cermets, Carbides, Hard Materials, and Minerals.", (2009).
72. Aliukov, S. and Osintsev, K., "Mathematical modeling of coal dust screening by means of sieve analysis and coal dust combustion based on new methods of piece-linear function approximation", *Applied Sciences (Switzerland)*, 11 (4): 1–15 (2021).
73. Sankhla, A. M., Patel, K. M., Makhesana, M. A., Giasin, K., Pimenov, D. Y., Wojciechowski, S., and Khanna, N., "Effect of mixing method and particle size on hardness and compressive strength of aluminium based metal matrix composite prepared through powder metallurgy route", *Journal Of Materials Research And Technology*, 18: 282–292 (2022).
74. Levitsky, I. and Tavor, D., "Improved atomization via a mechanical atomizer with optimal geometric parameters and an air-assisted component", *Micromachines*, 11 (6): 1–15 (2020).
75. Korim, N. S., Elsayed, A., and Hu, L., "Impacts of Lubricant Type on the Densification Behavior and Final Powder Compact Properties of Cu–Fe Alloy under Different Compaction Pressures", *Materials*, 15 (16): (2022).
76. Meshalkin, V. P. and Belyakov, A. V., "Methods used for the compaction and molding of ceramic matrix composites reinforced with carbon nanotubes", *Processes*, 8 (8): 1–37 (2020).
77. Nemati, N., Khosroshahi, R., Emamy, M., and Zolriasatein, A., "Investigation of microstructure, hardness and wear properties of Al-4.5wt.% Cu-TiC nanocomposites produced by mechanical milling", *Materials And Design*, 32 (7): 3718–3729 (2011).

78. Wang, W., Qi, H., Liu, P., Zhao, Y., and Chang, H., "Numerical simulation of densification of Cu–Al mixed metal powder during axial compaction", *Metals*, 8 (7): (2018).
79. G. Hammes, C. Binder, A. Galiotto, A. N. Klein, and H. A. Al-Qureshi, "No Title Relationship between Cold Isostatic Pressing and Uniaxial Compression of Powder Metallurgy", (2014).
80. Attia, U. M., "Cold-isostatic pressing of metal powders: a review of the technology and recent developments", *Critical Reviews In Solid State And Materials Sciences*, 0 (0): 1–24 (2021).
81. Atkinson, H. V and Davies, S., "Fundamental Aspects of Hot Isostatic Pressing : An Overview", m (December): (2000).
82. A. BALIN, ""Sıcak presleme tekniğiyle üretilen CoCrMo toz alaşımının sinterleme sıcaklığının mikroyapı üzerine etkisinin araştırılması/The invastigation of the effect of sintering heat on microstructure in CoCrMo powder alloy produced via hot pressing technique,"", (2011).
83. J. M. Torralba, "Improvement of mechanical and physical properties in powder metallurgy", 3: 281–294 (2014).
84. Corti, C. W., "Role of the Platinum Metals in the Activated Sintering of Refractory Metals.", *International Journal Of Refractory Metals And Hard Materials*, 6 (1): 28–34 (1987).
85. T. Goryczka and J. van Humbeeck, "NiTiCu shape memory alloy produced by powder technology", 456 (1–2): 194–200 .
86. R. M. German, "Sintering theory and practice.", (1996).
87. C. Wang et al., "Preparation of optimum degreasing–sintering process for metal–polymer blending low temperature 3D printing,", *Rapid Prototyp J*, (2018).
88. R. M. German, P. Suri, and S. J. Park, ""Liquid phase sintering,"", *J Mater Sci*, 44 (1): 1_39 (2009).
89. A. Nakajima and G. L. Messing, "Liquid-Phase Sintering of Alumina Coated with Magnesium Aluminosilicate Glass,", *Journal Of The American Ceramic Society*, 81 (5): 1163–1172 (1998).
90. J. L. Johnson and R. M. German, "Role of solid-state skeletal sintering during processing of Mo-Cu composites,", *Metallurgical And Materials Transactions A*, 32 (3): 605–613 (2001).
91. P. Lu, X. Xu, W. Yi, and R. M. German, "No Title Porosity effect on densification and shape distortion in liquid phase sintering,", *Materials Science And Engineering: A*, 318 (1_2): 111_121 (2001).

92. M. Pomeroy, "No", *Encyclopedia Of Materials: Technical Ceramics And Glasses*. Elsevier, (2021).
93. S.-J. L. Kang, "6 - NORMAL GRAIN GROWTH AND SECOND-PHASE PARTICLES," *In Sintering*, S.-J. L. Kang, Ed. Oxford: Butterworth-Heinemann, 91–96 (2005).
94. Oleiwi, F. H., "The Effect of Cr on Microstructure and Mechanical Properties of 316L Stainless Steel Used As Implant Material Produced By Powder Metallurgy 2023 Master Thesis Biomedical Engineering", (2023).
95. Liu, L., Ma, F., Kang, B., Liu, P., Qi, S., Li, W., Zhang, K., and Chen, X., "Preparation and mechanical and biological performance of the Sr-containing microarc oxidation layer on titanium implants", *Surface And Coatings Technology*, 463: 129530 (2023).
96. Zhai, W., Zhou, W., and Nai, S. M. L., "Grain refinement of 316L stainless steel through in-situ alloying with Ti in additive manufacturing", *Materials Science And Engineering: A*, 840: 142912 (2022).
97. Türkmen, M., Tanouz, A. M., Akgün, M., and Erden, M. A., "The Effect of Mn and Ti Ratio on Microstructure and Mechanical and Machinability Properties of 316 L Stainless Steel Used in Biomedical Applications", *Metals*, 13 (11): (2023).
98. Pandya, S., Ramakrishna, K. S., Raja Annamalai, A., and Upadhyaya, A., "Effect of sintering temperature on the mechanical and electrochemical properties of austenitic stainless steel", *Materials Science And Engineering: A*, 556: 271–277 (2012).
99. Uzunsoy, D., "Investigation of dry sliding wear properties of boron doped powder metallurgy 316L stainless steel", *Materials And Design*, 31 (8): 3896–3900 (2010).
100. Pavapootanont, G., Wongpanya, P., Viyanit, E., and Lothongkum, G., "Corrosion behavior of Ni steels in aerated 3.5-wt.% NaCl solution at 25°C by potentiodynamic method", *Engineering Journal*, 22 (4): 1–12 (2018).
101. Su, B., Wang, B., Luo, L., Wang, L., Su, Y., Xu, Y., Wang, F., Han, B., Huang, H., Guo, J., and Fu, H., "Effect of zirconium content on the microstructure and corrosion behavior of as-cast Ti-Al-Nb-Zr-Mo alloy", *Journal Of Materials Research And Technology*, 15: 4896–4913 (2021).

RESUME

Meftah Abdallah Abushaala ABUSHAALA graduated primary, elementary, and high school in Misrata city, after that, he started an undergraduate program at High Institute for Comprehensive Professions, Misurata, and was awarded a higher diploma in mechanical engineering in 2009. In February 2017, he graduated from The College of Technical sciences, Misurata, and awarded a vocational bachelor's degree in the Production and quality control division. Then, in 2022, he started at Karabük University to complete his M. Sc. education.